The biotic crisis across the Oceanic Anoxic Event 2: palaeoenvironmental inferences based in foraminifera and geochemical proxies from the South Iberian Palaeomargin

Reolid, M.[1], Sánchez-Quiñónez, C.A.[2], Alegret, L.[3], Molina, E.[3]

[1] Departamento de Geología and CEACT, Universidad de Jaén, Campus Las Lagunillas sn, 23071 Jaén, Spain

[2] Departamento de Geociencias, Universidad Nacional de Colombia, Bogotá, Carrera 30, nº 45-03, Colombia

[3] Departamento de Ciencias de la Tierra & IUCA, Universidad de Zaragoza, Pedro Cerbuna 12, 50009 Zaragoza, Spain

* *Corresponding author:* mreolid@ujaen.es

ABSTRACT

Open marine sediments of the Cenomanian/Turonian boundary are well exposed in the Spanish Baños de la Hedionda section (Betic Cordillera, South Iberian Palaeomargin). The analysis of foraminiferal assemblages and geochemical proxies allowed us to infer the impact of the oceanic anoxic event 2 (OAE2) in this area of the western Tethys. Three main intervals have been identified corresponding to different lithological units and biozones. (1) The top of the Capas Blancas Member (*Rotalipora cushmani* Biozone) represents the pre-extinction phase with diverse foraminiferal assemblages and a good water-column tiering, with well-oxygenated, oligotrophic deep-waters and oxygenated to poorly oxygenated, mesotrophic surface-waters. Foraminiferal opportunist species point to a minor event with dysoxic conditions preceding the OAE2. (2) The black radiolaritic shales (*Whiteinella archaeocretacea* Biozone) consist of a foraminiferal-barren interval, except for the lowermost centimeters where planktic surface-dweller opportunists are common. Redox sensitive elements (Cr/Al, V/Al, U/Th, Mo_{EF}, Mo_{aut}, U_{EF} and U_{aut}) and increased TOC values reflect oxygen depleted conditions related to the OAE2. The increase in P/Ti values at the base of this stratigraphic interval indicates an abrupt increase in productivity. High concentrations of radiolarians are congruent with high surface productivity probably related to changes in oceanic circulation and enhanced upwelling currents, as well as subsequent shallowing of the oxygen-minimum zone. The increase in Mo_{EF} and Mo_{aut} towards the top of the black radiolaritic shales indicates temporal euxinic conditions. (3) A slow recovery of foraminiferal assemblages is recorded at the base of the Boquerón Member (*Helvetoglobotruncana helvetica* Biozone), with seafloor recolonization by benthic foraminifera being recorded previous to the water column colonization by planktic forms, mainly by

intermediate to deep-dwellers typical of mesotrophic to oligotrophic waters. The subsequent proliferation of surface-dweller opportunists adapted to mesotrophic to eutrophic conditions, and the decrease in planktic foraminiferal diversity, may indicate the persistence of poorly oxygenated conditions in the water column.

Keywords: trophic conditions, redox conditions, foraminifera, OAE2, Cretaceous

1. Introduction

The Oceanic Anoxic Event 2 (OAE2) is represented by the worldwide deposition of organic-rich facies across the Cenomanian/Turonian (C/T) boundary. The OAE2 has been related to palaeoceanographic and climatic changes including greenhouse warming (e.g. Huber et al., 1999, 2002; Norris et al., 2002; Bornemann et al., 2008; Tsandev and Slomp, 2009; Monteiro et al., 2012; Pogge von Strandmann et al., 2013), a perturbation of the carbon cycle (e.g. Kuypers et al., 2002; Erba, 2004; Pogge von Strandmann et al., 2013), a sea-level transgression (Hallam, 1992), and a probable massive magmatic episode (e.g. Kuroda et al., 2007; Turgeon and Creaser, 2008; Erba et al., 2013). The planktic foraminiferal turnover (Coccioni and Luciani, 2004; Caron et al., 2006) includes the disappearance of the genus *Rotalipora* close to the OAE2 (e.g. Hart 1996, 1999; Nederbragt and Fiorentino, 1999; Keller et al., 2001; Coccioni and Luciani, 2004; Reolid et al., 2015). Planktic foraminifera are sensitive to temperature, chemical and trophic conditions of the seawater column and the ecostratigraphic analysis of their assemblages may be used to reconstruct palaeoceanographic changes across the OAE2 (e.g. Jarvis et al., 1988; Huber et al., 1999; Coccioni and Luciani, 2004; Gebhardt et al., 2004, 2010). In addition, the ecostratigraphic analysis of benthic foraminiferal assemblages is a useful tool to interpret fluctuations in oxygen and nutrient availability at the seafloor (e.g. Bernhard, 1986; Koutsoukos et al., 1990; Nagy, 1992; Jorissen et al., 1995; Van der Zwaan et al., 1999; Klein and Mutterlose, 2001; Reolid et al., 2008, 2012a, b). Some authors have interpreted an extinction event affecting benthic foraminiferal assemblages at the C/T boundary (e.g. Peryt and Lamolda, 1996; Kaiho, 1994, 1999; Peryt, 2004), but there is no unanimity (Holbourn and Kuhnt, 2002).

The analysis of redox-sensitive trace elements (such as Cr, Mo, and V, among others) has proved to be a useful tool for interpreting redox conditions during oceanic anoxic events. These elements are less soluble under reducing conditions, resulting in synsedimentary enrichments under oxygen-depleted conditions (Wignall and Myers, 1988; Calvert and Pedersen, 1993; Jones and Manning, 1994; Powell et al., 2003; Gallego-Torres et al., 2007; Reolid et al., 2012a, b, 2015). Geochemical proxies have also been successfully applied to

interpret palaeoproductivity, the most extensively used being Ba/Al and P/Ti ratios (e.g., Turgeon and Brumsack, 2006; Gallego-Torres et al., 2007; Robertson and Filippelli, 2008; Sun et al., 2008; Reolid and Martínez-Ruiz, 2012; Reolid et al., 2012a, b). The total organic carbon (TOC) has also been employed as an indirect palaeoproductivity proxy (e.g., Gupta and Kawahata, 2006; Su et al., 2008), although enhanced TOC contents may result from low bottom-water ventilation and oxygen depletion.

The aim of this work is to integrate planktic and benthic foraminiferal assemblages and geochemical proxies to determine the palaeoenvironmental turnover across the OAE2 in the Baños de la Hedionda section (Betic Cordillera, South Spain). The OAE2 and the Cenomanian-Turonian (C-T) transition are recorded in the Betic Cordillera, where studies on foraminifera, calcareous nannoplankton, radiolarian, and trace fossils have been carried out (e.g. Rodríguez-Tovar et al., 2009a, b; Sánchez-Quiñónez et al., 2010). Here we present the first integrated analysis of benthic and planktic foraminiferal assemblages and geochemical proxies across the C–T transition from the Baños de la Hedionda section.

2. Geological setting

The studied section (36º23’39’’N, 5º15’45’’W) is located in the Málaga province (South Spain), 1 km north from Manilva village (Fig. 1). From the geological point of view the studied section belongs to the Penibetic, i.e. to the External Zones of the Betic Cordillera (Fig. 1). The Betic Cordillera is the westernmost Alpine Mediterranean Chain together with the Rifian Cordillera in north Morocco. The Betic Cordillera is divided in internal and external zones, the last one formed by thin-skinned thrust sheets detached from their basement and consisting of thick successions of Triassic to Miocene sedimentary rocks (Vera, 2004). The Betic External Zones comprise the Prebetic and Subbetic, which constituted epicontinental and epioceanic environments respectively, from the Early Jurassic. The Baños de la Hedionda section is located in the westernmost part of the Internal Subbetic, also called the Penibetic, which constituted a moderately deep pelagic plateau located in the most distal part of the South Iberian palaeomargin (Martín-Algarra, 1987).

The Baños de la Hedionda section is located in the eastern limb of the N-S trending Canutos de la Utrera anticline, which constitutes a tectonic window among the Cretaceous-Tertiary turbiditic successions of the Campo de Gibraltar Flysch Complex. The succession is composed by thick limestones of the Líbar Group, surrounded by marly limestones and marls of the Espartina Group. The top of the Líbar Group is capped by a decimeter-thick pelagic limestone bed with phosphate deposits (stromatolites and macrooncoids) of the latest Valanginian–earliest Hauterivian (González-Donoso et al., 1983; Martín-Algarra and Vera,

1994; Martín-Algarra and Sánchez-Navas, 2000). The Espartina Group includes the Capas Blancas and the Capas Rojas formations, represented by scaglia-type facies consisting of white and red pelagic marly limestones and marls rich in chert nodules and layers, and characterised by the abundance of planktic foraminifera. The Capas Blancas Formation (~54 m thick) is subdivided in the Capas Blancas Member (~36 m thick) and Boquerón Member (~16 m thick) separated by a < 1.5 m thick bituminous interval that consists of black shales and black radiolaritic interlayers (Martín-Algarra, 1987).

The studied interval (Fig. 1c) is 6 m thick and belongs to the upper part of the Capas Blancas Formation. The lowermost 3.2 m consist of marls and marly-limestones with local chert nodules of the Capas Blancas Member (Figs. 1c and 2). These sediments are overlain by 1.45 m of black radiolaritic shales composed by thin laminated black clays and black radiolaritic cherts (Figs. 1c and 2). The uppermost 1.3 m of the studied section consist of white limestones with chert nodules and marls, and belong to the Boquerón Member (Fig. 1c and 2).

3. Material and methods

Lithofacies and microfacies were analysed by field observations and from a total of 19 thin sections and 2 polished slabs. Foraminiferal and geochemical analyses were conducted across the C-T transition. A total of 28 sampling levels were selected from this 6 m thick sedimentary succession (Fig. 1).

Micropalaeontological samples were disaggregated in water with diluted H_2O_2, washed through a 63 µm sieve, and dried at 50ºC. More endurated limestones were immersed in acetic acid (80%) during 1 h to 4 h, depending on the carbonate content, then washed through a 63 µm sieve, and dried at 50ºC. Quantitative studies were based on representative splits (using a modified Otto microsplitter) of over 300 specimens of benthic foraminifera larger than 63 µm and 300 specimens of planktic foraminifera larger than 100 µm per sample. The remaining residue was scanned for rare species. Simple diversity (number of species) and the Fisher-α diversity index (e.g. Murray, 1991) were calculated separately for benthic and planktic foraminiferal assemblages.

Whole-rock analyses of major elements were carried out in 28 samples using X-ray fluorescence (XRF) in a Philips PW 1040/10 spectrometer. The content of trace elements was determined using an inductively coupled plasma-mass spectrometer (ICP-MS Perkin Elmer Sciex-Elan 5000) at the Centro de Instrumentación Científica (CIC, Universidad de Granada). Instrumental error was ± 2% and ± 5% for respective elemental concentrations of 50 ppm and 5 ppm.

The contents in C, N and S, as well as the total organic carbon (TOC) content, were

analyzed with an Elemental Analyzer LECO CNS-TruSpec and an Inorganic Carbon Analyzer CM5240 UIC in the laboratories of the Centro Andaluz de Medio Ambiente (CEAMA, Granada). Total organic carbon was obtained as the difference between total carbon and total inorganic carbon; it was measured in mg and calculated as percentage of sample weight.

In order to compare trace-element proportions in samples with varying carbonate and clay contents, trace-element concentrations were normalized to aluminium content (Calvert and Pedersen, 1993). This technique avoids any lithological effects on trace or major element concentrations, assuming that Al content in sediments is heightened by alumino-silicates (e.g., Calvert, 1990). The study of palaeoproductivity was carried out applying two palaeoproductivity proxies, Ba/Al and P/Ti. To analyze palaeo-oxygenation, two redox proxies evaluating the relative increase of redox sensitive elements, Cr/Al and V/Al, were applied throughout the section as well as the enrichment factors of Mo and U, According to Zhou et al. (2012) and Tribovillard et al. (2012), the enrichment factors are calculated as Mo_{EF}= $[Mo/Al]_{sample}/[Mo/Al]_{PAAS}$ and U_{EF}= $[U/Al]_{sample}/[U/Al]_{PAAS.}$ The authigenic values of U and Mo were also calculated according to Zhou et al. (2012), as $Mo_{aut}=[Mo]_{sample}-[Mo]_{PAAS}/[Al]_{PAAS}*[Al]_{simple}$, $U_{aut}=[U]_{sample}-[U]_{PAAS}/[Al]_{PAAS}*[Al]_{simple}$.

4. Results

4.1. Microfacies

The top of the Capas Blancas Member corresponds to light (locally dark grey) marls and light grey marly limestones in decimentric beds with black chert nodules and interlayers (Fig. 2a). The microfacies range from mudstones to laminated packstones of planktic foraminifera and radiolarids (Fig. 2b).

The black radiolaritic shales interval is characterised by very dark coloured clay rich layers and radiolaritic layers (Fig. 2c). Thin lamination is persistent in both clay rich layers and radiolarites. The lower part (from 0 – 45 cm) is composed of black clayey radiolarites and dark grey or black silicified shales (both in beds < 5 cm thick). The middle interval (from 45 – 100 cm) contains 10 cm of black shales at the bottom, and is characterized by the dominance of black and grey radiolarites with well-laminated black shales interlayers. The upper interval (100 – 145 cm) contains alternations of black and grey radiolarites with black and dark grey shales (Figs 2c and d). The top of the black radiolaritic shale interval consists of a 4 cm thick horizon of green clays, overlain by the cherty limestone beds of the Boquerón Member.

The base of the Boquerón Member is more calcareous and rich in chert nodules than the top of the Capas Blancas Member, but radiolarids are very common (Figs. 2e and f).

4.2. Planktic foraminifera and biostratigraphy

For biostratigraphic assignments, we follow the planktic foraminiferal biozones proposed by Robaszynski and Caron (1995) for the Cretaceous in Europe and the Mediterranean. According to Ogg et al. (2012), the C/T boundary is located within the *Whiteinella archaeocretacea* Biozone.

The *Rotalipora cushmani, Whiteinella archaeocretacea* and *Helvetoglobotruncana helvetica* biozones have been recognized at the Baños de la Hedionda section. The *Rotalipora cushmani* Biozone (upper Cenomanian) corresponds to the studied interval of the Capas Blancas Member, except for its uppermost centimeters. This biozone is characterized by trochospiral keeled planktic forms such as *Rotalipora cushmani, Rotalipora monsalvensis, Thalmanninella greenhornensis, Talmannninella brotzeni, Parathalmanninella appenninica,* and *Thalmanninella deeckei*. The *Whiteinella archaeocretacea* Biozone includes the topmost centimeters of the Capas Blancas Member, the black radiolaritic shales and the first centimeters of the Boquerón Member. The most common species of this biozone are *Praeglobotruncana stephani, Praeglobotruncana gibba, Hedbergella delrioensis, Marginotruncana sigali*, and *Globigerinelloides bentonensis.* According to O'Dogherty (1994) and O'Dogherty et al. (2001) a sudden renewal of radiolarian species in this section delineates the boundary between *Guttacapsa biacuta* Biozone and *Alievium superbum* Biozone that correlated approximately to the *Whiteinella archaeocretacea* Biozone. The *Helvetoglobotruncana helvetica* Biozone (lower Turonian) includes the uppermost meter of the Boquerón Member. This biozone is characterized by the record of *Helvetoglobotruncana helvetica, Helvetoglobotruncana praehelvetica* and *Guembelitria cenomana*. Other characteristic species recorded within this biozone include *Marginotruncana marginata, Sigalitruncana marianosi* and *Whiteinella inornata*.

Planktic foraminiferal assemblages (Fig. 3) are abundant and diverse across the studied section except for the black radiolaritic shales unit, which is barren of foraminifera (Fig. 4). A total of 14 genera and 34 species have been recorded.

The Capas Blancas Member (samples BH-0 to BH-45) shows P/B values ranging from 97 to 99% (Fig. 4). The number of species of planktic foraminifera is high (17 to 22 species/sample) and the Fisher-α index of diversity ranges between 3.76 and 5.37 (Fig. 4). According to planktic morphogroups (Fig. 5), assemblages are dominated by trochospiral morphogroups in the Capas Blancas Member (83.4 to 94.2%), while planispiral planktic morphogroups make up between 4.7 and 13.1% of the assemblages (Fig. 6). Keeled trochospiral forms dominate over unkeeled forms. Biserial forms are a minor component of the assemblage (less than 5%). The most common species include *Praeglobotruncana stephani*, *Thalmanninella*

brotzeni, *Praeglobotruncana gibba*, *Rotalipora cushmani*, *Hedbergella delrioensis*, *Hedbergella planispira*, *Hedbergella simplex*, and *Globigerinelloides bentonensis*. The percentages of the species *Dicarinella algeriana*, *Hedbergella delrioensis*, *Thalmanninella greenhornensis* and *Whiteinella aprica* decrease towards the upper half of the Capas Blancas Member, while the percentages *Praeglobotruncana* (mainly *P. gibba* and *P. stephani*) and *Rotalipora cushmani* increase (Fig. 7). Two species disappear in the lower half of this member: *Dicarinella algeriana* reappears higher up in the section, and *Whiteinella aumalensis* has not been observed in any other samples across the studied section. All the identified species but four last occur in the uppermost sample of the Capas Blancas Member (Fig. 7).

The black radiolaritic shales constitute a barren interval except for the lowermost sample (BH-49), which contains 5 planktic foraminiferal species (*Globigerinelloides bentonensis Hedbergella delrioensis Marginotruncana sigali*, *Praeglobotruncana stephani* and *P. gibba*) but no benthic taxa. The low-diversity (Fisher-α = 2.62, Fig. 4) foraminiferal assemblage is dominated by trochospiral morphogroups (86.7%), mainly keeled forms, followed by planispiral morphogroups (13.3%, Fig. 6). Biserial and triserial planktic foraminifera are not recorded. *Globigerinelloides bentonensis* and *Hedbergella delrioensis* become more abundant in this sample with respect to the underlying Capas Blancas Member, and the species *Marginotruncana sigali* first occurs and makes up 26.7% of the assemblage (Fig. 7).

The lowermost 50 cm of the Boquerón Member are also barren of planktic foraminifera (Figs. 4, 6 and 7). The P/B ratio in the rest of this unit is high, but it drops down to 0% in sample BH-88 (Fig. 4). The number of planktic species ranges from 11 to 22 species/sample, and the Fisher-α index ranges between 2.99 and 5.48 (Fig. 4). Unkeeled trochospiral forms replace keel trochospiral ones in the upper half of this member (Fig. 6). Biserial and triserial morphogroups are a minor component of the assemblages, and planispiral forms are recorded only in the lowermost sample (BH-83). *Whiteinella baltica*, *Praeglobotruncana stephani*, *Praeglobotruncana gibba*, *Hedbergella delrioensis* and *Dicarinella algeriana* are the most common species (Fig. 7). The lower half of the Boquerón Member is characterized by high percentages of *Dicarinella algeriana*, which was scarcely recorded in the Capas Blancas Member. Other species of *Dicarinella* and the genera *Globoheterohelix* and *Guembelitria* first occur at the base of the Boquerón Member. The middle part of the Boquerón Member is characterized by increasing proportions of *Hedbergella delrioensis* and *Whiteinella baltica* (Fig. 7).

4.3. Benthic foraminifera

A total of 53 genera and 69 species of benthic foraminifera have been recorded in the Baños de la Hedionda section (Fig. 8). Calcareous taxa dominate the assemblages (up to 93%) except for sample BH-23 in the Capas Blancas Member, where agglutinated forms make up to 52.4% of the assemblage. There are no benthic foraminifera in the black radiolaritic shales nor in the lowermost 10 cm of the Boquerón Member (Fig. 9).

The number of benthic foraminiferal species ranges from 17 to 38 in the Capas Blancas Member, and the Fisher-α diversity index ranges from 5.14 to 14.62 (Fig. 4). Among benthic morphogroups, the biconvex trochospiral (e.g., *Gyroidinoides globosus*, *Charltonina australis*, *Charltonina* sp., *Gavelinella cenomanica* and *Gavelinella* sp.) and cylindrical elongated morphogroups (e.g., *Tritaxia gaultina*, *Laevidentalina* spp., *Praebulimina* spp. and *Marsonella oxycona*) dominate (Fig. 9). Pseudospheric forms such as *Ammosphaeroidina* spp. are also common in the Capas Blancas Member. The epifaunal forms are more abundant than infuanl ones (Fig. 10). A significant increase in the percentages of *Charltonina australis* (17.4%, BH-17), *Gavelinella* spp. (22.8%, BH-17) and *Glomospira* spp. (23.8%, BH-23) has been observed between meters 1 to 1.5 m in the Capas Blancas Member (Fig. 9).

Assemblages recorded immediately above the barren interval in the Boquerón Member are significantly different from those in the Capas Blancas Member. The number of species increases from the base (9, sample BH-81) to the top (21, sample BH-88) of the Boquerón Member, and the Fisher-α index increases from 2.95 to 4.95 (Fig. 4). These values are lower than in the Capas Blancas Member. Assemblages in the Boquerón Member are dominated by biconvex trochospiral (*Gyroidinoides beisseli* and *Gyroidinoides globosus*), cylindrical (*Praebulimina* spp., *Tritaxia gaultina* and *Pleurostomella* spp.) and planoconvex trochospiral morphogroups (*Stensioeina exsculpta*). Now, infaunal forms are dominant respect to epifaunal ones (Fig. 10). The lower part of this member is characterized by high proportions of species that were scarcer in the Capas Blancas Member, such as *Gyroidinoides beisseli* (24.6%), *Praebulimina* spp. (35.0%), *Stensioeina exsculpta* (17.5%), and *Pleurostomella* spp. (5.3%) (Fig. 9). Taxa such as *Tappanina* sp. (21.0%), *Gaudryina* spp., *Gavelinella* spp. and *Lenticulina* spp. are recorded immediately above the lowermost sample of the Boquerón Member (Fig. 9).

4.4. Geochemistry

4.4.1. Redox proxies

The analysis of redox proxies allowed us to subdivide the studied section into three intervals that correspond to the three stratigraphic units (Fig. 11): the Capas Blancas Member (*Rotalipora cushmani* Biozone), the black radiolaritic shales (*W. archaeocretacea* Biozone), and the Boquerón Member (topmost of *W. archaeocretacea* and base of the *H. helvetica* Biozone).

The Capas Blancas Member (*R. cushmani* Biozone) is characterized by very low values of Cr/Al, U/Th, V/Al, Mo_{EF}, $Mo_{aut.}$, U_{EF} and $U_{aut.}$ ratios, followed by a sudden increase in U/Th, V/Al, U_{EF} and $U_{aut.}$ ratios in the black radiolaritic shales (*W. archaeocretacea* Biozone), with the highest values recorded in the upper part of the black radiolaritic shales (Fig. 11). A gradual increase in Cr/Al, Mo_{EF}, and $Mo_{aut.}$ ratios within the black radiolaritic shales leads to the highest values in the upper part of this unit. U_{EF} and Mo_{EF} reach significantly high values in the black radiolaritic shales (7.46 and 22.38, respectively); according to Tribovillard et al. (2012), an elemental enrichment factor > 3 is considerable, and > 10 is considered as a strong enrichment.

At the base of the Boquerón Member limestones (*Helvetoglobotruncana helvetica* Biozone), the redox ratios decrease down to the original values recorded in the Capas Blancas Member (Fig. 11).

4.4.2. Palaeoproductivity proxies and TOC

The selected palaeoproductivity proxies and TOC show the most significant changes in the black radiolaritic shales (Fig. 12), except for the Ba/Al ratio which shows a prominent peak in the lower part of the Capas Blancas Member (sample BH-7). A peak in the P/Ti ratio has been recorded towards the base of the black radiolaritic shales coincident with a strong decrease in the $\%CaCO_3$ (Fig. 12), which shows very low values in this unit (0.5 – 3.6 wt.%). The TOC and TS reach the maximum values in the upper part of the black radiolaritic shales (4.8 wt.% and 2.2 wt.% respectively, sample BH-69), in the same horizon where maximum values in the redox proxies Cr/Al, V/Al, U_{EF} and $U_{aut.}$ have been recorded (Figs. 11 and 12). TOC and TS return to lower values and the $\%CaCO_3$ increases at the base of the Boquerón Member (*Helvetoglobotruncana helvetica* Biozone, Fig. 12).

5. Palaeoenvironmental interpretation

5.1. Capas Blancas Member: Pre-extinction phase

The Capas Blancas Member is characterised by the dominance of planktic foraminifera, with a good water-column tiering including potential deep-dweller specialists (*Rotalipora* and *Thalmanninella*), intermediate-dwellers (e.g. *Praeglobotruncana*) and potentially surface-dweller opportunists (e.g. *Hedbergella* and *Globigerinelloides*). This assemblage composition indicates well-oxygenated, oligotrophic deep-waters and oxygenated to poorly oxygenated, mesotrophic surface-waters (Fig. 13). However, some minor changes may be described in the planktic assemblages. A gradual increase in the percentage of keeled forms (mainly *Thalmanninella brotzeni*, *Praeglobotruncana stephani* and *Rotalipora cushmani*), parallel to a

decrease in unkeeled trochospiral forms (mainly *Hedbergella delrioensis* and *Whiteinella aprica*) in the lower part of the Capas Blancas Member (Fig. 6) may be related to a lithological change from limestones to marls and marly limestones. This change is correlative with an increase in Ba/Al ratio (Fig. 11), which is a palaeoproductivity proxy (Reolid and Martínez-Ruiz, 2012). However, the P/Ti ratio, another palaeoproductivity proxy, does not show any significant fluctuations.

Benthic assemblages from the Capas Blancas are slightly dominated by epifaunal forms (e.g. *Gyroidinoides globosus* and *Charltonina australis*) but also contain some components of shallow (mainly *Laevidentalina* spp., *Ammosphaeroidina* spp., and *Marsonella oxycona*) and deep (*Tritaxia gaultina*) infaunal microhabitats (Fig. 10). This assemblage composition points to low mesotrophic conditions in the sea-bottom microhabitats because composition of morphogroups is equilibrated (Fig. 13), except in isolated simples where epifaunal forms are higher than 50%. Typical benthic forms indicative of oxygen poor, eutrophic conditions (such as *Praebulimina*, *Pleurostomella*, *Tappanina*, *Glomospira* and *Gavelinella*; e.g. Koutsoukos et al., 1990; Coccioni et al., 1993; Widmark, 2000; Gebhardt et al., 2010; Reolid et al., 2015) are scarcely represented (Fig. 9). The marly interval of this member, however, contains quantitative peaks in the abundance of *Charltonina australis*, *Gavelinella* spp., *Globorotalites* sp., *Pleurostomella* spp. *Spiroplectammina roemeri*, *Glomospira* spp. and *Praebulimina* spp. (samples BH-17 to BH-23) which point to decreased sea-bottom water oxygenation (Fig. 13), as *Gavelinella*, *Globorotalites*, *Glomospira*, *Praebulimina* and *Pleurostomella* are indicatives of low oxygen conditions (e.g. Gebhardt et al., 2010; Reolid et al., 2015). *Gavelinella* spp. is a low-oxygen tolerant genus (Sliter, 1975; Koutsaoukos et al., 1990; Gertsch et al., 2010), and it occurs in shales with high organic matter levels (Holbourn et al., 2001). *Globorotalites* has been observed to peak under stressful conditions at the seafloor after the Cretaceous/Paleogene impact event (Alegret, 2007; Alegret et al., 2012). The interpretation of dysoxic conditions is supported by a small peak in the U_{EF} (Fig. 11). This minor event within the *Rotalipora cushmani* Biozone consists of an ecological replacement of opportunistic taxa, being *Gavelinella* the first colonizer and *Glomospira* and *Praebulimina* the last ones reaching the peaks of their maximum percentages (Fig. 9). Among planktic assemblages, the relative abundance of the deep-dweller specialist *Rotalipora cushmani* and the surface-dweller opportunists *Hedbergella* and *Heterohelix* increase in coincidence with this minor event (Fig. 7).

An increase in the percentage of *Charltonina*, *Glomospira*, *Lenticulina* and *Praebulimina* is recorded immediately above this short interval of dysoxic sea-bottom water conditions (Fig. 9). These genera are not dominant but point to unfavorable conditions in spite of the fact that redox and palaeoproductivity proxies do not change significantly (Figs. 11 and

12). The increase of opportunistic forms prior to an anoxic event and prior to associated variations in geochemical proxies was also documented across the Toarcian Oceanic Anoxic Event by Reolid et al. (2012). A significant decrease in the diversity of benthic foraminifera occurs towards the top of the Capas Blancas Member, and is congruent with the progress of the unfavorable conditions at the seafloor.

Ichnofabric analysis carried out by Rodríguez-Tovar et al. (2009a) revealed the occurrence of *Chondrites*, *Planolites*, *Trichichnus* and *Palaeophycus* at the top of the Capas Blancas Member. These authors interpreted a well-oxygenated environment punctuated by short intervals of oxygen-depleted conditions.

5.2. Black radiolaritic shales: Oceanic Anoxic Event 2

The lack of benthic foraminifera in the black radiolaritic shales, and the occurrence of planktic foraminifera only in the lowermost sample (BH-49), point to adverse conditions during sedimentation of the black shales. Low-diversity planktic assemblages from sample BH-49 (Fig. 4) are dominated by surface-dweller opportunists (*Hedbergella delrioensis* and *Globigerinelloides bentonensis*, Fig. 5), which indicate poorly oxygenated waters and eutrophic conditions (Fig. 13). But in this sample also persists non-opportunist intermediate-dwellers (*Praeglobotruncana gibba* and *Praeglobotruncana stephani*), and abundant *Marginotruncana*. No deep-dweller specialists such as *Rotalipora* and *Thalmanninella* have been found in this assemblage. Apart from sample BH-49, the black radiolaritic shales are barren of foraminifera, suggesting adverse conditions in the water column. Huber et al. (1999) interpreted increased pCO_2 and deep water warming which may have caused a breakdown in the vertical tiering of the water column and could explain the extinction of deeper dwelling planktic species.

Redox conditions in the water column and at the seafloor may be inferred from the analysis of redox-sensitive trace elements (Cr, Mo, U and V), which tend to co-precipitate with sulfides (mainly pyrite) and are usually not remobilized during diagenesis in the absence of post-depositional replacement of oxidizing agents (Tribovillard et al., 2006). The enhancement in redox sensitive elements (Cr/Al, V/Al, U/Th, Mo_{EF}, Mo_{aut}, U_{EF} and U_{aut}) points to depleted oxygen conditions during deposition of the black radiolaritic shales (Figs. 11 and 13). U-based proxies (U_{EF}=7.46 and U_{aut}= 10.07) and increased TOC values (4.84 wt.%) point to depleted oxygen conditions in the lower part of the water column (Fig. 13).

The P/Ti ratio is a commonly used proxy for productivity (Latimer and Filippelli, 2001; Robertson and Filippelli, 2008; Reolid et al., 2012a, b, 2015). Increased values are related to a higher phosphorous supply to the seafloor derived from biological processes, not from terrigenous components (Latimer and Filippelli, 2001; Flores et al., 2005; Sen et al., 2008). At

Baños de la Hedionda section, the increase in P/Ti values at the base of the *W. archaeocretacea* Biozone indicates an abrupt increase in productivity (Fig. 12). Such an increase in the P/Ti ratio was also identified at the base of this biozone in the Tunisian Oued Bahloul section in the base of the *W. archaeocretacea* (Reolid et al., 2015). Mort et al. (2007) suggested that the increase in P-accumulation rates coinciding with the OAE2 may be related to an overall increase in surface-water productivity. However, in Baños de la Hedionda section maximum values of P/Ti ratio do not coincide with maximum values of TOC or U_{EF} (Figs. 11 and 12). The Ba/Al ratio, which has also been used as a palaeoproductivity proxy (Sun et al., 2008; Reolid and Martínez-Ruiz, 2012; Reolid et al., 2012a, b), does not show any significant fluctuations in the black shales interval.

Therefore, the initial increase in opportunist planktic foraminifera typical of poorly oxygenated environments and eutrophic conditions, and the disappearance of deep-dweller specialists (e.g. *Rotalipora*) and benthic forms is congruent with the debut of the OAE2 as well as with the high P/Ti values. Persistent oxygen restricted conditions are confirmed by the relatively higher TOC values (reaching 4.84 wt.%), which point to higher accumulation of organic matter derived from surface primary productivity than in the Capas Blancas Member (Schlanger and Jenkyns, 1976; Arthur et al., 1990; Ingall et al., 1993; Van Cappellen and Ingall, 1994; Mort et al., 2007). TOC values have been used in the literature (e.g., Calvert and Fontugne, 2001; Gupta and Kawahata, 2006; Plewa et al., 2006; Su et al., 2008; Reolid et al., 2012a) as an indirect palaeoproductivity proxy when TOC is related to phytodetritus associated with phytoplankton or dinoflagellate remains. Nevertheless, because high TOC values may result from low bottom-water ventilation and oxygen depletion, they are not necessarily related to high surface productivity. According to Tribovillard et al. (2006), the TOC is generally proportional to surface-water productivity and constitutes a useful palaeoproductivity proxy in spite of certain complications attributable to efficient organic recycling, export productivity, delivery to the sediment-water interface and final burial.

Radiolarians are a major component of the black radiolaritic shales (Fig. 2d) and indicate abnormally high surface productivity. High concentrations of radiolarians have been typically documented from black shales related to the OAE2 in northern European sections (e.g., Jarvis et al., 1988; Scopelliti et al., 2004; Kędzierski et al., 2012; Uchman et al., 2013), which are often barren of planktic foraminifera. According to Jarvis et al. (1988), major changes in oceanic circulation during the C-T transition enhanced upwelling currents, with nutrient-rich deep-waters emerging towards the surface. Moreover, abundance of radiolarians in the same sediments is congruent with shallowing of the oxygen-minimum zone caused by enhanced ocean-surface productivity.

In the Recent marine environments there is a positive correlation between TOC and total sulphur (TS) mainly coming from pyrite (Berner and Raiswell, 1983). Under depleted oxygen conditions (dysoxic or anoxic), the organic matter decays at the seafloor or in the sediment-water interface, resulting in increased reduction rates of sulphate, increased H_2S in the sediment pore-water, and the progressive shallowing of the redox boundary within the sediment. The H_2S reacts with the detritic Fe and forms pyrite. In this sense, the TS in the black shales interval is congruent with the highest TOC values and the oxygenation decrease indicated by V/Al and Cr/Al ratios (Figs. 11 and 12).

High Mo_{EF} and Mo_{aut} values require the presence of H_2S (euxinic conditions) (Tribovillard et al., 2012; Zhou et al., 2012). The increase in Mo_{EF} and Mo_{aut} across the black shales indicates a decrease in oxygen availability towards euxinia (Fig. 13). Other authors have reported euxinic conditions from the OAE2 (e.g., Wang et al., 2001; Scopelliti et al., 2004; Reolid et al., 2015). The progressive accentuation of oxygen-depleted conditions from the base of the black shales upwards is compatible with the disappearance of planktic taxa that flourished at the beginning of the eutrophic conditions (e.g., *Hedbergella* and *Globigerinelloides*).

Marine anoxia during the OAE2 is thought to have been related to enhanced biological productivity (e.g. Monteiro et al., 2012; Pogge von Strandmann et al., 2013). Uranium and organic matter in the sediment are related, as uranium may form a complex with dissolved fulvic acid in hemipelagic sediments (Nagao and Nakashima, 1992). In this sense, high values for U_{EF} and U_{aut} are congruent with the high values of TOC. In open-ocean systems with suboxic bottom waters, U_{aut} enrichment is greater than that of Mo_{aut} because U_{aut} accumulation begins at the Fe (II)-Fe (III) redox boundary (Zhou et al., 2012), while Mo_{aut} accumulation becomes more relevant as waters become euxinic. Higher values of U_{aut} recorded in the lower part of the black shale interval are congruent with anoxic conditions not only at the sea-bottom waters but also in the deeper layers of the water column, where deep dwellers such as *Rotalipora* inhabited. However, the upper part of the black shales (BH-69 to BH-79) presents higher values of Mo_{aut} than U_{aut} and indicates euxinic conditions.

Based ichnologic analysis, Rodríguez-Tovar et al. (2009a) interpreted anoxic conditions during deposition of the black radiolaritic shales, with interruptions by short dysaerobic to oxic periods as suggested by the occurrence of such ichnotaxa as *Chondrites*, *Planolites*, *Thalassinoides* and rare *Zoophycos* in greenish or light grey silicified shales.

5.3. Boquerón Member: recovery

Foraminiferal assemblages from the Boquerón Member significantly differ from those recorded below the OAE2. The lowermost sample of the Boquerón Member only contains

benthic foraminifera, while planktic foraminifera reappear 26 cm above the base of this member, where the first occurrence of new species of *Dicarinella* (*D. canaliculata*, *hagni* and *D. imbricata*) has been observed. *D. algeriana*, a species that has not been recorded in the upper part of the Capas Blancas Member, dominates the assemblages in the lowermost part of the *Helvetoglobotruncana praehelvetica* Biozone (Fig. 7). The genus *Dicarinella* has been interpreted as an intermediate-dweller typical of oxygenated mesotrophic environments (Coccioni and Luciani, 2004; Fig. 5). The assemblages also contain common intermediate to deep-dweller forms typical of oxygenated, mesotrophic environments such as *Praeglobotruncana gibba*, *P. stephani* and *Helvetoglobotruncana praehelvetica*. Opportunist surface-dweller forms typical of oxygenated to poorly oxygenated waters with mesotrophic to eutrophic conditions are also recorded (e.g., *Hedbergella*, *Whiteinella*, *Guembelitria* and *Heterohelix*). The opportunistic surface dweller *Whiteinella* progressively proliferated during the *Helvetoglobotruncana helvetica* Biozone. *Guembelitria* is interpreted as an opportunist surface-dweller adapted to poorly oxygenated, eutrophic waters (Coccioni and Luciani, 2004; Reolid et al., 2015) or to variable salinity and nutrient levels (Keller and Pardo, 2004). The deep-dweller specialists (*Rotalipora*, *Thalmanninella*) are definitively extinct and there are no genera occupying this ecologic niche (Fig. 7).

Diversity values of benthic foraminifera are lower than in the Capas Blancas Member. Assemblages are dominated by opportunistic species of the genera *Praebulimina*, *Gyroidinoides*, *Tappanina* and *Pleurostomella* (e.g., Peryt and Lamolda, 1996). The clear dominance of *Praebulimina* spp. immediately above the extinction interval suggests that they may have behaved as disaster species (Peryt and Lamolda, 1996; Reolid et al., 2015). Buliminids are considered to be indicators of high-food and/or low oxygenation at the seafloor in the modern oceans (e.g., Fontanier et al., 2002; Gooday, 2003). Some species of *Gyroidinoides* have been interpreted as opportunists (e.g. Peryt and Lamolda, 1996). *Tappanina* is a biserial, infaunal species that has been reported from dysoxic facies in highly eutrophic environments (e.g. Eicher and Worstell, 1970; Gustafsson et al., 2003; Friedrich and Erbacher, 2006). Species of *Praebulimina*, *Pleurostomella* and *Tappanina* have been reported from dysoxic facies in highly eutrophic environments and high organic-matter fluxes (e.g. Eicher and Worstell, 1970; Coccioni et al., 1993; Widmark, 2000; Gustafsson et al., 2003; Gebhardt et al., 2004; Friedrich and Erbacher, 2006; Friedrich et al., 2009; Reolid et al., 2015). Moreover, the dominance of infaunal taxa in the Boquerón Member supports the interpretation of eutrophic and low oxygen conditions at the seafloor (Jorissen et al., 1995). Similarly, dysoxic conditions have also been inferred from infaunal-dominated assemblages immediately above the OAE2 event in the Spanish Menoyo section (Peryt and Lamolda, 1996).

In contrast, redox proxies do not indicate oxygen depleted conditions in the Boquerón Member. We conclude that the palaeoenvironmental perturbation related to the OAE2 (recorded in the foraminiferal-barren interval of the black radiolaritic shales) induced slow recovery of the foraminiferal assemblages, especially affecting benthic foraminifera which display low diversity and are dominated by opportunistic species. Detailed analysis of the benthic assemblages shows a succession of abundance peaks that represent the first stages of seafloor recolonization after the OAE2, which correspond to the ecological replacement of mainly opportunistic foraminifera (abundance peaks of *Gyroidinoides beisseli* and *Stensioeina exsculpta* in BH-81, followed by peaks of *Praebulimina* sp. and *Gyroidinoides globosus* in BH-83, and *Tappanina* and *Pleurostomella* in BH-87). The first colonizers were epifaunal forms, and these were followed by peaks of infaunal opportunists, indicating the persistence of adverse conditions at the seafloor.

The first stages of seafloor recolonization by benthic foraminifera occurred previous to the water column colonization by planktic forms, mainly by intermediate to deep-dwellers typical of mesotrophic to oligotrophic waters (*Dicarinella algeriana*, *Praeglobotruncana stephani*, *P. gibba* and *Helvetoglobotruncana praehelvetica*). These data indicate that the recovery of environmental conditions began in deep and intermediate waters. However, the subsequent proliferation of surface-dweller opportunists (*Whiteinella baltica*, *Hedbergella delrioensis*, *H. simplex*) adapted to mesotrophic to eutrophic conditions, and the decrease in planktic foraminiferal diversity, may indicate the return to poorly oxygenated conditions in the water column during the *Helvetoglobotruncana helvetica* Biozonen (Fig. 13).

According to Rodríguez-Tovar et al. (2009a), trace fossils from the Boquerón Member (mainly *Chondrites* and *Planolites*) suggest the recovery to pre-OAE conditions, although they identified several intervals with oxygen-depleted conditions.

6. Conclusions

The detailed analysis of foraminiferal assemblages and geochemical proxies from the Baños de la Hedionda section (South Iberian Palaeomargin) allowed us to identify the impact of the OAE2 in this area of the western Tethys.

The Capas Blancas Member represents the pre-extinction phase with diverse foraminiferal assemblages and a good water-column tiering, with well-oxygenated, oligotrophic deep-waters and oxygenated to poorly oxygenated, mesotrophic surface-waters. A minor event with dysoxic conditions preceding the OAE2 is indicated by quantitative peaks of benthic (*Gavelinella*, *Glomospira* and *Praebulimina*) and planktic (*Hedbergella* and *Heterohelix*) opportunists.

The lack of foraminifera in the black radiolaritic shales (*Whiteinella archaeocretacea* Biozone), points to adverse conditions. Planktic foraminifera, mainly surface-dweller opportunists, are only recorded in the lowermost centimeters of the black shales. The enhancement in redox sensitive elements (Cr/Al, V/Al, U/Th, Mo_{EF}, Mo_{aut}, U_{EF} and U_{aut}) and increased TOC values point to depleted oxygen conditions. The increase in P/Ti values at the base of this stratigraphic interval indicates an abrupt increase in productivity. Therefore, the initial increase in opportunist planktic foraminifera typical of poorly oxygenated environments and eutrophic conditions, and the disappearance of deep-dweller specialists (e.g. *Rotalipora*) and benthic forms is congruent with the debut of the OAE2 as well as with the high redox and palaeoproductivity proxies. High concentrations of radiolarians indicate abnormally high surface productivity probably related to changes in oceanic circulation and enhanced upwelling currents, as well as subsequent shallowing of the oxygen-minimum zone. The increase in Mo_{EF} and Mo_{aut} indicates a decrease in oxygen availability towards euxinia in the upper part of the black radiolaritic shales.

The first centimeters of the Boquerón Member (*Helvetoglobotruncana helvetica* Biozone) only contain benthic foraminifera, while planktic forms reappear 26 cm above the base of this member. Foraminiferal assemblages are less diverse than in the Capas Blancas Member. Planktic foraminifera are represented by intermediate-dwellers typical of oxygenated mesotrophic environments and opportunist surface dwellers typical of oxygenated to poorly oxygenated waters with mesotrophic to eutrophic conditions. Benthic assemblages are dominated by opportunistic species that indicate dysoxic conditions above the OAE2 event.

The palaeoenvironmental perturbation related to the OAE2 induced slow recovery of the foraminiferal assemblages, especially affecting benthic foraminifera which display low diversity and are dominated by opportunistic species. However, the first stages of seafloor recolonization by benthic foraminifera occurred previous to the water column colonization by planktic forms, mainly by intermediate to deep-dwellers typical of mesotrophic to oligotrophic waters. These data indicate that the recovery of environmental conditions began in deep and intermediate waters. The subsequent proliferation of surface-dweller opportunists adapted to mesotrophic to eutrophic conditions, and the decrease in planktic foraminiferal diversity, may indicate the return to poorly oxygenated conditions in the water column.

Acknowledgements

We thank Agustín Martín Algarra (Universidad de Granada) and Luis O'Dogherty (Universidad de Cádiz) for priceless collaboration during the sampling campaign. This study

has been conducted within the framework of the Projects CGL2011-23077, CGL2011-22912, CGL2012-33281 and RYC-2009-04316 of the Spanish Ministry of Science and Technology (FEDER funds), P11-RNM-7408 (Junta de Andalucía), and the Consolidated Group E05 funded by the Government of Aragón. Sánchez-Quiñónez, C.A. thanks the Fundación Carolina (Spain) for finantial support during this research stay at Zaragoza University.

References

Alegret, L., 2007. Recovery of the deep-sea floor after the Cretaceous/Paleogene boundary event: the benthic foraminiferal record in the Basque-Cantabrian basin and in South-eastern Spain. Palaeogeography, Palaeoclimatology, Palaeoecology 255, 181–194.

Alegret, L., Thomas, E., Lohmann, K.C., 2012. End-Cretaceous marine mass extinction not caused by productivity collapse. Proceedings of the National Academy of Sciences 109, 728–732

Arthur, M.A., Jenkyns, H.C., Brumsack, H.J., Schlanger, S.O., 1990. Stratigraphy, geochemistry, and paleoceanography of organic carbon-rich Cretaceous sequences. In: Ginsburg, R.N., Beaudoin, B., (eds.), Cretaceous Ressources, Events and Rhythms: Background and Plans for Research, NATO ASI series, pp. 75–119.

Bernhard, J.M., 1986. Characteristic assemblages and morphologies of benthic foraminifera from anoxic, organic rich deposits: Jurassic trough Holocene. Journal of Foraminiferal Research 16, 207–215.

Bornemann, A., Norris, R.D., Friedrich, O., Beckmann, B., Schouten, R., Sinninghe-Damste, J., Vogel, J., Hofmann, P., Wagner, T., 2008. Isotopic evidence for glaciation during the Cretaceous super-greenhouse. Science 319, 951–954.

Calvert, S.E., 1990, Geochemistry and origin of the Holocene sapropel in the Black Sea. In Ittekkot, V., Kempe, S., Michaelis, W., and Spitzy, A. (eds.), Facets of Modern Biogeochemistry, Springer, Berlin, pp. 326–352.

Calvert, S.E., Fontugne, M.R., 2001. On the late Pleistocene-Holocene sapropel record of climatic and oceanographic variability in the eastern Mediterranean. Paleoceanography 16, 78–94.

Calvert, S.E., Pedersen, T.F., 1993. Geochemistry of recent oxic and anoxic marine sediments: Implications for the geological record. Marine Geology 113, 67–88.

Caron, M., 1983. La spéciation chez les Foraminifères planctiques: une réponse adaptée aux contraintes de l´environnement. Zitteliana 10, 671–676.

Coccioni, R., Fabbrucci, L., Galeotti, S., 1993. Terminal Cretaceous deep-water benthic foraminiferal decimation, survivorship and recovery at Caravaca (SE Spain). Paleopelagos 3, 3–24.

Coccioni, R., Luciani, V., 2004. Planktonic foraminifera and environmental changes across the Bonarelli Event (OAE2, Latest Cenomanian) in its type area: a high-resolution study from the Tethyan reference Bottaccione section (Gubbio, Central Italy). Journal of Foraminiferal Research 34, 109–129.

Eicher, D.L., Worstell, P., 1970. Cenomanian and Turonian foraminfiera from the Great Plains, United States. Micropaleontology 16, 269–324.

Erba, E., 2004. Calcareous nannofossils and Mesozoic oceanic anoxic events. Marine Micropaleontology 52, 85–106.

Erba, E., Bottini, C., Faucher, G., 2013. Cretaceous large igneous provinces: The effects of submarine volcanism on calcareous nannoplankton. Mineralogical Magazine 77, p. 1044.

Flores, J.A., Sierro, F.J., Filippelli, G.M., Barcena, M.A., Pérez-Folgado, M., Vázquez, A., Utrilla, R., 2005. Surface water dynamics and phytoplankton communities during deposition of cyclic late Messinian sapropel sequences in the western Mediterranean. Marine Micropaleontology 56, 50–79.

Fontanier, C., Jorissen, F.J., Licari, L., Alexandre, A., Anschutz, P., Carbonel, P., 2002. Live benthic foraminiferal faunas from the Bay of Biscay: faunal density, composition and microhabitats. Deep-Sea Research. Part 1. Oceanographic Research Papers 49, 751–785.

Friedrich, O., Erbacher, J., 2006. Benthic foraminiferal assemblages from Demerara Rise (ODP Leg 207, western Tropical Atlantic): possible evidence for a progressive opening of the Equatorial Atlantic Gateway. Cretaceous Research 27, 377–397.

Friedrich, O., Erbacher, J., Wilson, P.A., Moriya, K., Mutterlose, J., 2009. Paleoenvironmental changes across the Mid Cenomanian Event in the tropical Atlantic Ocean (Demerara Rise, ODP Leg 207) inferred from benthic foraminiferal assemblages. Marine Micropaleontology 71, 28–40.

Gallego-Torres, D., Martínez-Ruiz, F., Paytan, A., Jiménez-Espejo, F.J., Ortega-Huertas, M., 2007. Pliocene–Holocene evolution of depositional conditions in the eastern Mediterranean: Role of anoxia vs. productivity at 632 time of sapropel deposition. Palaeogeography, Palaeoclimatology, Palaeoecology 246, 424–439.

Gebhardt, H., Kuhnt, W., Holbourn, A., 2004. Foraminiferal response to sea level change, organic flux and oxygen deficiency in the Cenomanian of the Tarfaya Basin, southern Morocco. Marine Micropaleontology 53, 133–157.

Gebhardt, H., Friederich, O., Schenk, B., Fox, L., Hart, M., Wagreich, M., 2010. Paleoceanographic changes at the northern Tethyan margin during the Cenomanian-Turonian Oceanic Anoxic Event (OAE2). Marine Micropaleontology 77, 25–45.

Gertsch, B., Keller, G., Adatte, T., Berner, Z., Kassab, A.S., Tantawy, A.A.A., El-Sabbagh, A.M., Stueben, D., 2010. Cenomanian-Turonian transition in a shallow water sequence of the Sinai, Egypt. International Journal of Earth Sciences 99, 165–182.

González-Donoso, J.M., Linares, D., Martín-Algarra, A., Rebollo, M., Serrano, F., Vera, J.A., 1983. Discontinuidades estratigráficas durante el Cretácico en el Penibético (Cordillera Bética). Estudios Geológicos 39, 71–116.

Gooday, A., 2003. Benthic foraminifera (Protista) as tools in deep-water palaeoceanography: environmental influences on faunal characteristics. Advances in Biology 46, 1–90

Gupta, L.P., Kawahata, H., 2006. Downcore diagenetic changes in organic matter and implications for paleoproductivity estimates. Global and Planetary Change 53, 122–136.

Gustafsson, M., Holbourn, A., Kuhnt, W., 2003. Changes in Northeast Atlantic temperature and carbon flux during the Cenomanian/Turonian paleoceanographic event: the Goban Spur stable isotope record. Palaeogeography, Palaeoclimatology, Palaeoecology 201, 51–66.

Hallam, A., 1992. Phanerozoic sea level changes. Columbia Press, New York, 266 pp.

Hart, M.B., 1996. Recovery of the food chain after the late Cenomanian extinction event. In: Hart, M.B. (ed.), Biotic recovery from Mass Extinction Events. Geological Society of London Sp. Publ. 102, 265–277.

Hart, M.B., 1999. The evolution and diversity of Cretaceous planktonic foraminiferida. Geobios 32, 247–255.

Holbourn, A., Kuhnt, W., 2002. Cenomanian-Turonian palaeoceanographic change on the Kerguelen Plateau a comparison with Northern Hemisphere records. Cretaceous Research 23, 333–349.

Holbourn, A., Kuhnt, W., Erbacher, J., 2001. Benthic foraminifers from lower Albian black shales (Site 1049, ODP leg 171): evidence for a non ‘uniformitarian’ record. Journal of Foraminiferal Research 31, 60–74.

Huber, B.T., Leckie, R.M., Norris, R.D., Bralower, T.J., CoBabe, E., 1999. Foraminiferal assemblages and stable isotopic change across the Cenomanian-Turonian boundary in the subtropical North Atlantic. Journal of Foraminiferal Research 29, 392-417.

Huber, B.T., Norris, R.D., McLeod, K.G., 2002. Deep-sea paleotemperature record of extreme warmth during the Cretaceous. Geology 30, 123–126.

Ingall, E.D., Bustin, R.M., Van Cappellen, P., 1993. Influence of water column anoxia on the burial and preservation of carbon and phosphorus in marine shales. Geochimica et Cosmochimica Acta 57, 303–316.

Jarvis, I., Carson, G.A., Cooper, M.K.E., Hart, M.B., Leary, P.N., Tocher, B.A., Horne, D., Rosenfeld, A., 1988. Microfossil assemblages and the Cenomanian-Turonian (Late Cretaceous) oceanic anoxic event. Cretaceous Research 9, 3-103

Jones, B.A., Manning, D.A.C., 1994. Comparison of geochemical indices used for the interpretation of paleoredox conditions in ancient mudstones. Chemical Geology 111, 111–129.

Jorissen, F.J., De Stigter, H.C., Widmark, J.G.V., 1995. A conceptual model explaining benthic foraminiferal habitats. Marine Micropaleontology 26, 3–15.

Kaiho, K., 1994. Planktonic and benthic foraminiferal extinction events during the last 100 m.y. Palaeogeography, Palaeoclimatology, Palaeoecology 111, 45–71.

Kaiho, K., 1999. Evolution in the test size of deep-sea benthic foraminifera during the past 120 m.y. Marine Micropaleontology 37, 53–65.

Keller, G., Han, Q., Adatte, T., Burns, S.J., 2001. Paleoenvironment of the Cenomanian-Turonian transition at Eastbourne, England. Cretaceous Research 22, 391–322.

Keller, G., Pardo, A., 2004. Age and environment of the Cenomanian-Turonian global stratotype section and point at Pueblo, Colorado. Marine Micropaleontology 51, 95–128.

Kędzierski, M., Machaniec, E., Rodríguez-Tovar, F.J., Uchman, A., 2012. Bio-events, foraminiferal and nannofossil biostratigraphy of the Cenomanian/Turonian boundary interval in the Subsilesian Nappe, Rybie section, Polish Carpathians. Cretaceous research 35, 181-198.

Klein, C., Mutterlose, J., 2001. Benthic foraminifera: indicators for a long-term improvement of living conditions in the late Valanginian of the NW German Basin. Journal of Micropalaeontology 20, 81–95.

Koutsoukos, E.A.M., Leary, P.N., Hart, M.B., 1990. Latest Cenomanian-earliest Turonian low-oxygen tolerant benthonic foraminifera: a case-study from the Serpige basin (NE Brazil) and the western Anglo-Patis basin (southern England). Palaeogeography, Palaeoclimatology, Palaeoecology 77, 145-177.

Kuroda, J., Ogawa, N.O., Tanimizu, M., Coffin, M.T., Tokuyama, H., Kitazato, H., Ohkouchi, N., 2007. Contemporaneous massive subaerial volcanism and late Cretaceous Oceanic Anoxic Event 2. Earth Planetary Science Letters 256, 211–223.

Kuypers, M.M.M., Pancost, R.D., Nijenhuis, I.A., Sinninghe-Damste, J.S., 2002. Enhanced productivity led to increased organic carbon burial in the euxinic North Atlantic Basin during the late Cenomanian oceanic anoxic event. Paleoceanography 17, 1051.

Latimer, J.C., Filippelli, G.M., 2001. Terrigenous input and paleoproductivity in the Southern Ocean. Paleoceanography 16, 627–643.

Martín-Algarra, A., 1987. Evolución Geológica Alpina del Contacto entre las Zonas Internas y las Zonas Externas de la Cordillera Bética, PhD Thesis Universidad de Granada, 1171 pp.

Martín-Algarra, A., Sánchez-Navas, A., 2000. Bacterially mediated authigenesis in Mesozoic stromatolites from condensed pelagic sediments (Betic Cordillera, Southern Spain). In: Glenn, C.R., Lucas, J., Prév□t-Lucas, L. (eds.), Marine Authigenesis: From Global to Microbial. SEPM Special Publication 66, 499–525.

Martín-Algarra, A., Vera, J.A., 1994. Mesozoic pelagic phosphate stromatolites from the Penibetic (Betic Cordillera, Southern Spain). In: Bertrand-Sarfati, J., Monty, C. (eds.), Phanerozoic Stromatolites II, Kluwer Academic Publishers, New York, p. 345–391.

Monteiro, F.M., Pancost, R.D., Ridwell, A., Donnadieu, Y., 2012. Nutrients as the dominant control on the spread of anoxia and euxinia across the Cenomanian-Turonian oceanic anoxic event (OAE2): model-data comparison. Paleoceanography 27, PA4209.

Mort, M., Adatte, T., Föllmi, K.B., Keller, G., Steinmann, P., Matera, V., Berner, Z., Stüben, D., 2007. Phosphorous and the roles of productivity and nutrient recycling during oceanic event 2. Geology 35, 483–486.

Murray, J.W., 1991. Ecology and palaeoecology of benthic foraminifera. Longman, Harlow, 397 pp.

Nagao, S., Nakashima, S., 1992. Possible Complexation of Uranium with Dissolved Humic Substances in Pore Water of Marine-Sediments. Science of the Total Environment 118, 439–447.

Nagy, J., 1992. Environmental significance of foraminiferal morphogroups in Jurassic North Sea deltas. Palaeogeography, Palaeoclimatology, Palaeoecology 95, 111–134.

Nederbragt, A.J., Fiorentino, A., 1999. Stratigraphy and paleoceanography of the Cenomanian-Turonian Boundary Event in Oued Mellegue, north-western Tunisia. Cretaceous Research 20, 47–62.

Norris, R.D., Bice, K.L., Magno E.A., Wilson, P.A., 2002. Jiggling the tropical thermostat in the Cretaceous hothouse. Geology 30, 299–302.

O'Dogherty, L., 1994. Biochronology and paleontology of Mid-Cretaceous radiolarians from Northern Apennines (Italy) and Betic Cordillera (Spain). Mémoires de Géologie, Lausanne, 21, 1-415.

O'Doghery, L., Martín-Algarra, A., Gursky, H.J., Aguado, R., 2001. El horizonte radiolaritico-bituminoso del límite Cenomaniense-Turoniense en la Zona Subbética. Geotemas 3, 249-252.

Peryt, D., 2004. Benthic foraminiferal response to the Cenomanian-Turonian and Cretaceous-Paleogene boundary events. Przegla□d Geologiczny 52, 827–832.

Peryt, D., Lamolda, M., 1996. Benthonic foraminiferal mass extinction and survival assemblages from the Cenomanian-Turonian Boundary Event in the Menoyo section, northern Spain. Geological Society, London, Special Publications 102, 245–258.

Plewa, K., Meggers, H., Kasten, S., 2006. Barium in sediments off northwest Africa: A tracer for palaeoproductivity or meltwater events? Paleoceanography 21, PA2015.

Pogge von Strandmann, P.A.E., Jenkyns, H.C., Woodfine, R.G., 2013. Lithium isotope evidence for enhanced weathering during Oceanic Anoxic Event 2. Nature Geoscience 6, 668–672.

Powell, W.G., Johston, P.A., Collom, C.J., 2003. Geochemical evidence for oxygenated bottom waters during deposition of fossiliferous strata of the Burgess Shale Formation. Palaeogeography, Palaeoclimatology, Palaeoecology 201, 249–268.

Reolid, M., Martínez-Ruiz, F., 2012. Comparison of benthic foraminifera and geochemical proxies in shelf deposits from the Upper Jurassic of the Prebetic (southern Spain). Journal of Iberian Geology 38, 449–465.

Reolid, M., Rodríguez-Tovar, F.J., Nagy, J., Olóriz, F., 2008. Benthic foraminiferal morphogroups of mid to outer shelf environments of the Late Jurassic (Prebetic Zone, Southern Spain): Characterisation of biofacies and environmental significance. Palaeogeography, Palaeoclimatology, Palaeoecology 261, 280–299.

Reolid, M., Rodríguez-Tovar, F.J., Marok, A., Sebane, A., 2012a. The Toarcian Oceanic Anoxic Event in the Western Saharan Atlas, Algeria (North African Paleomargin): role of anoxia and productivity. Geological Society of America Bulletin 124, 1646–1664.

Reolid, M., Rodríguez-Tovar, F.J., Nagy, J., 2012b. Ecological replacement of Valanginian agglutinated foraminifera during a maximum flooding event in the Boreal realm (Spitsbergen). Cretaceous Research 33, 196–204.

Reolid, M., Sánchez-Quiñónez, C.A., Alegret, L., Molina, E., 2015. Palaeoenvironmental turnover across the Cenomanian-Turonian transition in Oued Bahloul, Tunisia: Foraminifera and geochemical proxies. Palaeogeography, Palaeoclimatology, Palaeoecology 417, 491-510.

Robaszynski, F., Caron, M., 1995. Foraminifères planctoniques du Crétacé: Commentaire de la zonation Europe-Méditerranée. Bulletin de la Société géologique de France 166(6), 681-692.

Robertson, A.K., Filippelli, G.M., 2008. Paleoproductivity variations in the eastern equatorial Pacific over glacial timescales: American Geophysical Union Fall Meeting 2008, Abstract PP33C-1576.

Rodríguez-Tovar, F.J., Uchman, A., Martín-Algarra, A., 2009a. Oceanic anoxic event at the Cenomanian-Turonian boundary interval (OAE-2): ichnological approach from the Betic Cordillera, southern Spain. Lethaia 42, 407-417.

Rodríguez-Tovar, F.J., Uchman, A., Martín-Algarra, A., O'Dogherty, L., 2009b. Nutrient spatial variation during intrabasinal upwelling at the Cenomanian-Turonian oceanic anoxic event in the westernmost Tethys: An ichnological and facies approach. Sedimentary Geology 215, 83-93.

Sánchez-Quiñónez, C.A., Alegret, L., Aguado, R., Delgado, A., Larrasoaña, J.C., Martín-Algarra, A., O'Dogherty, L., Molina, E., 2010. Foraminíferos del tránsito Cenomaniense-Turoniense en la sección de El Chorro, Cordillera Bética, sur de España. Geogaceta 49, 23-26.

Schlanger, S.O., Jenkyns, H.C., 1976. Cretaceous oceanic anoxic events, causes and consequences. Geologie en Mijnbouw 55, 179–184.

Scopelliti, G., Bellanca, A., Coccioni, R., Luciani, V., Neri, R., Baudin, F., Chiari, M., Marcucci, M., 2004. High-resolution geochemical and biotic records of the Tethyan 'Bonarelli Level' (OAE2, latest Cenomanian) from the Calabianca-Guidaloca composite section, northwestern Sicily, Italy. Palaeogeography, Palaeoclimatology, Palaeoecology 208, 293–317.

Sen, A.K., Filippelli, G.M., Flores, J.A., 2008. An application of wavelet analysis to palaeoproductivity records from the Southern Ocean. Computers & Geosciences 35, 1445–1450.

Sliter, W.V., 1975. Foraminiferal life and residue assemblages from Cretaceous slope deposits. Geological Society of America Bulletin 86, 897–906.

Su, W., Wang, Y., Cramer, B.D., Munnecke, A., Li, Z., Fu, L., 2008. Preliminary estimation of palaeoproductivity via TOC and habitat types: which method is more reliable? A case study on the Ordovician/Silurian transitional black shales of the Upper Yangtze Platform, South China. Journal of China University of Geosciences 19, 534–548.

Sun, Y.B., Wu, F., Clemens, S.C., Oppo, D.W., 2008. Processes controlling the geochemical composition of the South China Sea sediments during the last climatic cycle. Chemical Geology 257, 234–249.

Thierry, J., 2000. Middle Callovian (157–155 Ma). In: Dercourt, J., Gaetani, M., Vrielynck, B., Barrier, E., Biju-Duval, B., Brunet, M-F., Cadet, J.P., Crasquin, S., Sandulescu, M. (Eds.), Atlas Peri-Tethys palaeogeographical maps. CCGM/CGMW, Paris, pp. 71–97.

Tribovillard, N., Algeo, T., Lyons, T., Riboulleau, A., 2006. Trace metals as palaeoredox and palaeoproductivity proxies: an update. Chemical Geology 232, 12–32.

Tribovillard, N., Algeo, T.J., Baudin, F., Riboulleau, A., 2012. Analysis of marine environmental conditions based on molybdenum-uranium covariation – Applications to Mesozoic paleoceanography. Chemical Geology 324–325, 46–58.

Tsandev, I., Slomp, C.P., 2009. Modeling phosphorous cycling and carbon burial during Cretaceous Oceanic Anoxic Events. Earth and Planetary Science Letters 286, 71–79.

Turgeon, S.C., Brumsack, H.J., 2006. Anoxic vs dysoxic events reflected in sediment geochemistry during the Cenomanian-Turonian Boundary Event (Cretaceous) in the Umbria-Marche basin of central Italy. Chemical Geology 234, 321–339.

Turgeon, S.C., Creaser, R.A., 2008. Cretaceous oceanic anoxic event 2 triggered by a massive magmatic episode. Nature 454, 323–326.

Uchman, A., Rodríguez-Tovar, F.J., Machaniec, E., Kędzierski, M., 2013. Ichnological characteristics of Late Cretaceous hemipelagic and pelagic sediments on a submarine high around the OAE-2 event: A case from the Rybie section, Polish Carpathians. Palaeogeography, Palaeoclimatology, Palaeoecology 370, 222-231.

Van Cappellen, P., Ingall, E.D., 1994. Benthic phosphorus regeneration, net primary production, and ocean anoxia—A model of the coupled marine biogeochemical cycles of carbon and phosphorus. Paleoceanography 9, 677–692.

Van der Zwaan, G.J., Duijnstee, I.A.P., Den Dulk, M., Ernst, S.R., Jannink N.T., Kouwenhoven, T.J., 1999. Benthic foraminifers: proxies or problem? A review of paleoecological concepts. Earth-Science Reviews 46, 213–236.

Vera, J.A. (coord.), 2004. Zonas Externas Béticas. In: J.A. Vera (Ed.), Geología de España. SGE-IGME, Madrid, 354-389.

Wang, C.S., Hu, X.M., Jansa, L., Wan, X.Q., Tao, R., 2001. The Cenomanian-Turonian anoxic event in southern Tibet. Cretaceous Research 22, 481–490.

Widmark, J.G.V., 2000. Biogeography of terminal Cretaceous benthic foraminifera: deep-water circulation and trophic gradients in the deep South Atlantic. Cretaceous Research 21 (2-3), 367-379.

Widmark, J.G.V., Speijer, R.P., 1997. Benthic foraminiferal faunas and trophic regimes at the terminal Cretaceous Tethyan seafloor. Palaios 12, 354–371.

Wignall, P.B., Myers, K.J., 1988. Interpreting the benthic oxygen levels in mudrocks: a new approach. Geology 16, 452–455.

Zhou, L., Wignall, P.B., Su, J., Feng, Q., Xie, S., Zhao, L., Huang, J., 2012. U/Mo ratios and $\delta^{98/95}$Mo as local and global redox proxies during mass extinction events. Chemical Geology 324-325, 99–197.

Appendix 1. Planktic foraminiferal species

Dicarinella algeriana (Caron, 1966)

Dicarinella canaliculata (Reuss, 1854)

Dicarinella hagni (Scheibnerova, 1962)

Dicarinella imbricata (Mornod, 1950)

Globigerinelloides bentonensis (Morrow, 1934)

Globigerinelloides ultramicrus (Subbotina, 1949)

Globoheterohelix paraglobulosa Georgescu & Huber, 2009

Guembelitria cenomana (Keller, 1935)

Hedbergella delrioensis (Carsey, 1926)

Hedbergella planispira (Tappan, 1940)

Hedbergella simplex (Morrow, 1934)

Helvetoglobotruncana helvetica (Bolli, 1945)

Helvetoglobotruncana praehelvetica (Trujillo, 1960)

Heterohelix moremani (Cushman, 1938)

Heterohelix reussi (Cushman, 1938)

Marginotruncana marginata (Reuss, 1845)

Marginotruncana sigali (Reichel, 1950)

Parathalmanninella appenninica (Renz, 1936)

Praeglobotruncana delrioensis (Plummer, 1931)

Praeglobotruncana gibba Klaus, 1960

Praeglobotruncana stephani (Gandolfi, 1942)

Rotalipora cushmani (Morrow, 1934)

Rotalipora monsalvensis (Mornod, 1950)

Schackoina cenomana (Shacko, 1897)

Sigalitruncana marianosi (Douglas, 1969)

Thalmanninella brotzeni Sigal, 1948

Thalmanninella deeckei (Franke, 1925)

Thalmanninella greenhornensis (Morrow, 1934)

Whiteinella aprica (Loeblich & Tappan, 1961)

Whiteinella archaeocretacea Pesaggno, 1967

Whiteinella aumalensis (Sigal, 1952)

Whiteinella baltica Douglas and Rankin, 1969

Whiteinella brittonensis (Loeblich and Tappan, 1961)

Whiteinella inornata (Bolli, 1957)

Appendix 2. Benthic foraminiferal species

Ammodiscus spp.

891 *Aragonia* sp.

892 *Ammosphaeroidina* spp.

893 *Arenobulimina* spp.

894 *Astacolus crepidularis* (Roemer, 1842)

895 *Astacolus gratus* (Reuss, 1863)

896 *Astacolus* spp.

897 *Bathysiphon* spp.

898 *Charltonina australis* Scheibnerová, 1978

899 *Charltonina* sp.

900 *Clavulinoides* sp.

901 *Conorotalites* sp.

902 *Coryphostoma* spp.

903 *Dorothia pupa* (Reuss, 1860)

904 *Dorothia* spp.

905 *Ellipsoidella* sp.

906 *Ellipsodimorphina* sp.

907 *Epistomina* sp.

908 *Epistomina spinulifera* (Reuss, 1862)

909 *Frondicularia* sp.

910 *Gaudryina pyramidata* Cushman, 1926

911 *Gaudryina* spp.

912 *Gavelinella cenomanica* (Brotzen, 1945)

913 *Gavelinella* spp.

914 *Glandulina* sp.

915 *Globorotalites sp.*

916 *Globulina* sp.

917 *Glomospira* spp.

918 *Glomospirella* sp.

919 *Gubkinella graysonensis* (Tappan, 1940)

920 *Gyroidinoides beisseli* (White, 1928)

921 *Gyroidinoides globosus* (Hagenow, 1842)

922 *Gyroidinoides* sp.

923 *Gyroidinoides subglobosus* Dailey, 1970

924 *Hemirobulina* sp.

925 *Hyperammina* sp.

926 *Laevidentalina* spp.

Lagena sp.

Lenticulina rotulata (Lamarck, 1804)

Lenticulina spp.

Lenticulina truncata (Reuss, 1851)

Lingulina sp.

Marginulina sp.

Marginulinopsis sp.

Marssonella oxycona (Reuss, 1860)

Oolina spp.

Patellina sp.

Plectina pinswangensis Hagn, 1953

Pleurostomella spp.

Praebulimina spp.

Pyrulina spp.

Pyrulinoides spp.

Quadrimorphina sp.

Ramulina spp.

Rhabdammina sp.

Saracenaria sp.

Spiroplectammina roemeri Lalicker, 1935

Spiroplectammina sp.

Spiroplectammina spectabilis (Grzybowski, 1898)

Stensioeina exsculpta (Reuss, 1860)

Stensioeina granulata (Olbertz, 1942)

Stensioeina sp.

Tappanina selmensis (Cushman, 1933)

Tappanina sp.

Textularia sp.

Tristix sp.

Tritaxia gaultina (Morozova, 1948)

Vaginulinopsis sp.

Valvulineria sp.

Figure caption.

Fig. 1. (a) Geological setting of the Betic Cordillera, (b) detailed geological setting of the studied section (star) close to Manilva village, (c) Baños de la Hedionda section including the lithostratigraphic units, foraminiferal biozones and location of the samples.

Fig. 2. Macroscopic view of the differentiated lithostratigraphic units and the respective microfacies. Capas Blancas Member (a) and (b), black radiolaritic shales (c) and (d), and Boquerón Member (e) and (f). Scale bar 1 mm.

Fig. 3. Planktic foraminiferal species in the Los Baños de la Hedionda section: **1-2** *Rotalipora monsalvensis* (BH-0). **3-4** *Parthalmanninella appenninica* (BH-5, BH-7). **5** *Marginotruncana* sp. (BH-17). **6** *Whiteinella archaeocretacea* (BH-17). **7** *Praeglobotruncana delrioensis* (BH-40). **8-9** *Praeglobotruncana gibba* (BH-45). **10-11** *Dicarinella hagni* (BH-83). **12** *Dicarinella algeriana* (BH-83). **13** *Dicarinella imbricata* (BH-83). **14** *Dicarinella canaliculata* (BH-83). **15** *Shackoina cenomana* (BH-83). **16-17** *Guembelitria cenomana* (BH-83). **18** *Dicarinella* sp. (BH-89). **19-20** *Helvetoglobotruncana helvetica* (BH-89). **21** *Marginotruncana marginata* (BH-89). **22- 23** *Dicarinella hagni* (BH-89). Scale bars: 0.1 mm.

Fig. 4. Stratigraphic distribution of planktic/benthic ratio (P/B) and diversity of planktic and benthic foraminifera.

Fig. 5. Planktic foraminiferal morphogroups and inferred life style including redox and trophic requirements based on Hart and Bailey (1979), Hart (1999), Keller et al. (2001), Coccioni and Luciani (2004) and Reolid et al. (2015).

Fig. 6. Stratigraphic distribution of planktic foraminiferal morfogroups.

Fig. 7. Stratigraphic distribution of planktic foraminiferal taxa.

Fig. 8. Benthic foraminiferal species in the Los Baños de la Hedionda section: **1** *Spiroplectammina roemeri* (BH-0). **2** *Plectina pinswagensis* (BH-0). **3** *Ammodiscus* sp. (BH-0). **4** *Arenobulimina* sp. (BH-0). **5** *Lingulina* sp. (BH-0). **6** *Saracenaria* sp. (BH-0). **7** *Hemirobulina* sp**.** (BH-0). **8** *Tristix* sp. (BH-0). **9** *Stensioeina exsculpta*. **10-11** *Charltonina australis* (BH-0). **12** *Bolivinopsis spectabilis* (BH-1). **13** *Ammosphaeroidina* sp. (BH-1). **14** *Gaudryina pyramidata* (BH-3). **15-16-17** *Gyroidinoides globosus* (BH-18). **18** *Gyroidinoides beisseli* (BH-18). **19-20** *Valvulineria* sp. (BH-24). **21-22** *Globorotalites* sp. (BH-25). **23-24** *Gyroidinoides subglobosus* (BH-88). Scale bars: 0.1 mm.

Fig. 9. Stratigraphic distribution of selected benthic foraminiferal species.

Fig. 10. Stratigraphic distribution of benthic foraminifera according to the inferred microhabitat.

Fig. 11. Stratigraphic fluctuations of geochemical redox proxies and U- and Mo-based proxies (enrichment factor and authigenic content).

Fig. 12. Stratigraphic distribution of CO_3Ca, total sulphur (TS), total organic carbon (TOC), and geochemical palaeoproductivity proxies (Ba/Al and P/Ti ratios).

Fig. 13. Evolution of trophic conditions, productivity and oxygenation in the water column and at the seafloor (sea-bottom waters) inferred from foraminiferal assemblages and geochemical proxies.

Figure 01
Click here to download high resolution image

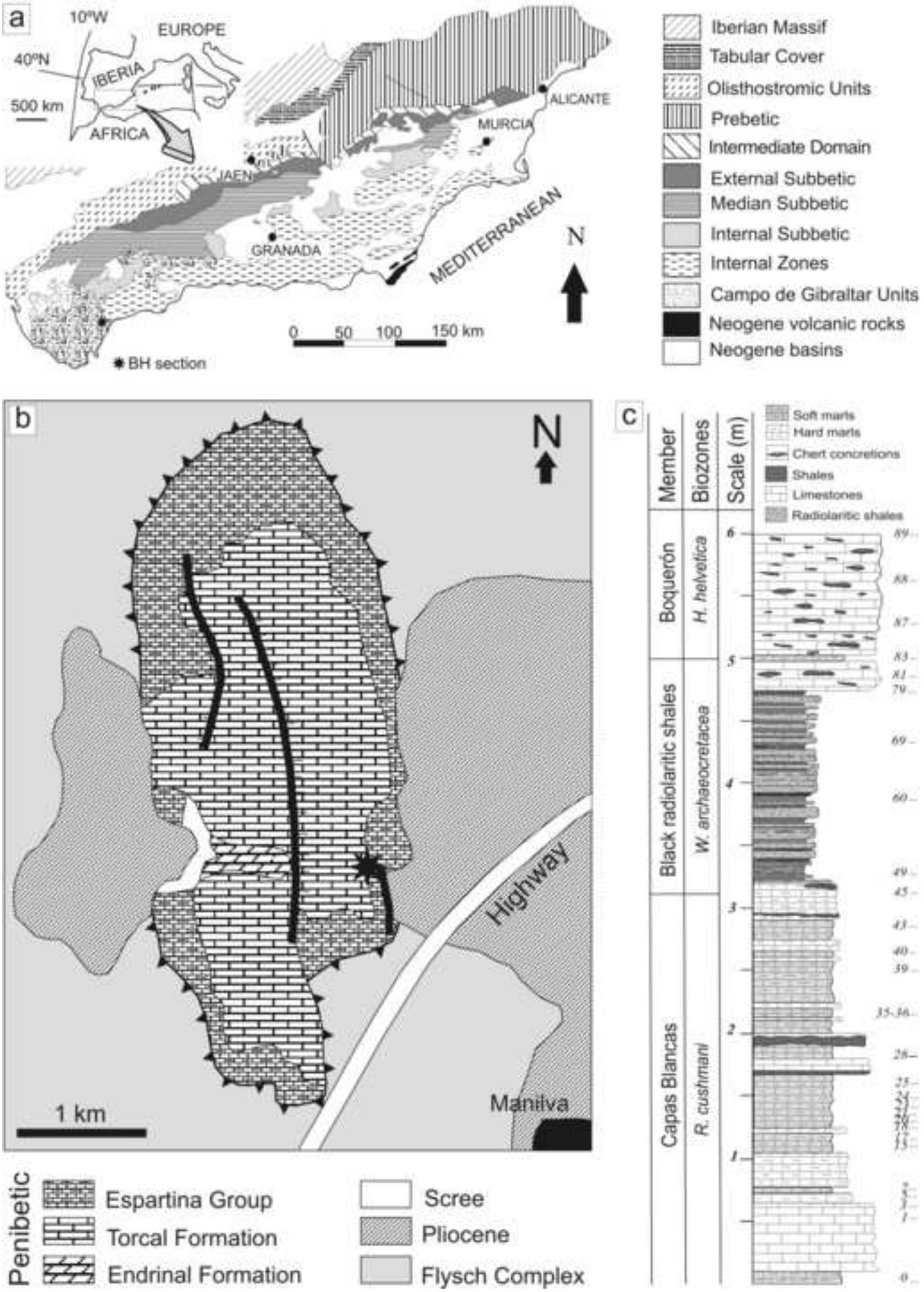

Figure 02
Click here to download high resolution image

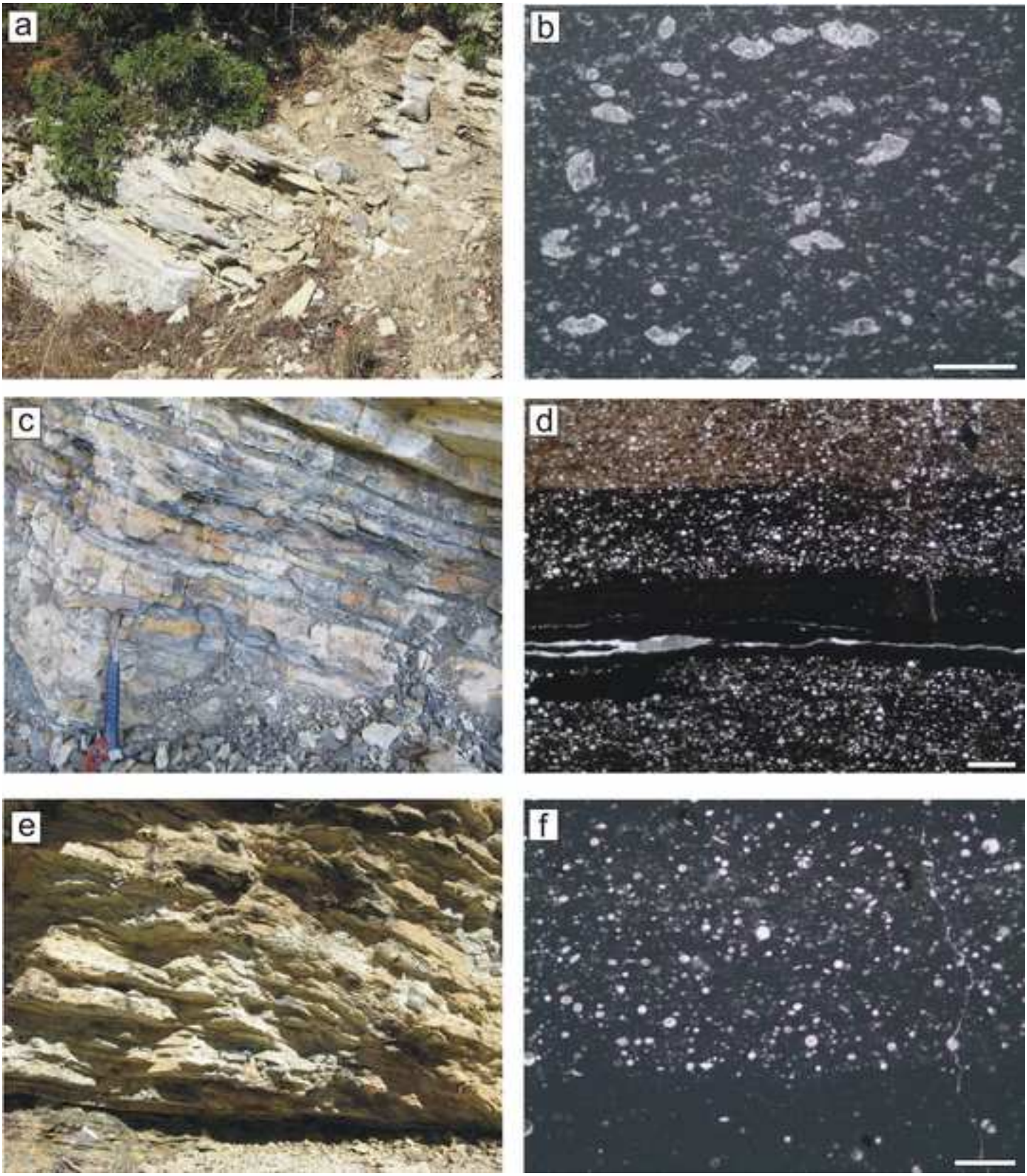

Figure 03
Click here to download high resolution image

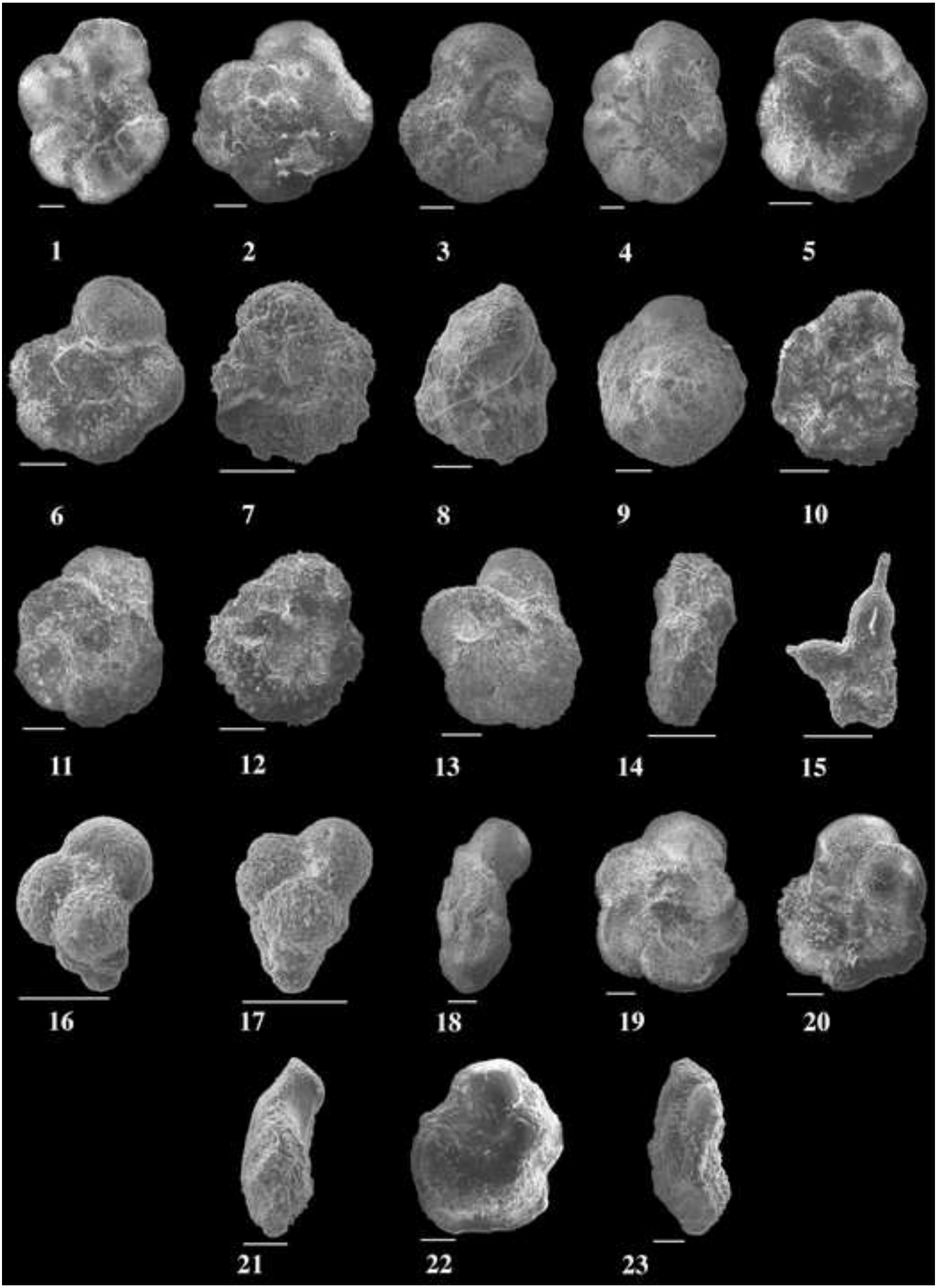

Figure 03

Click here to download high resolution image

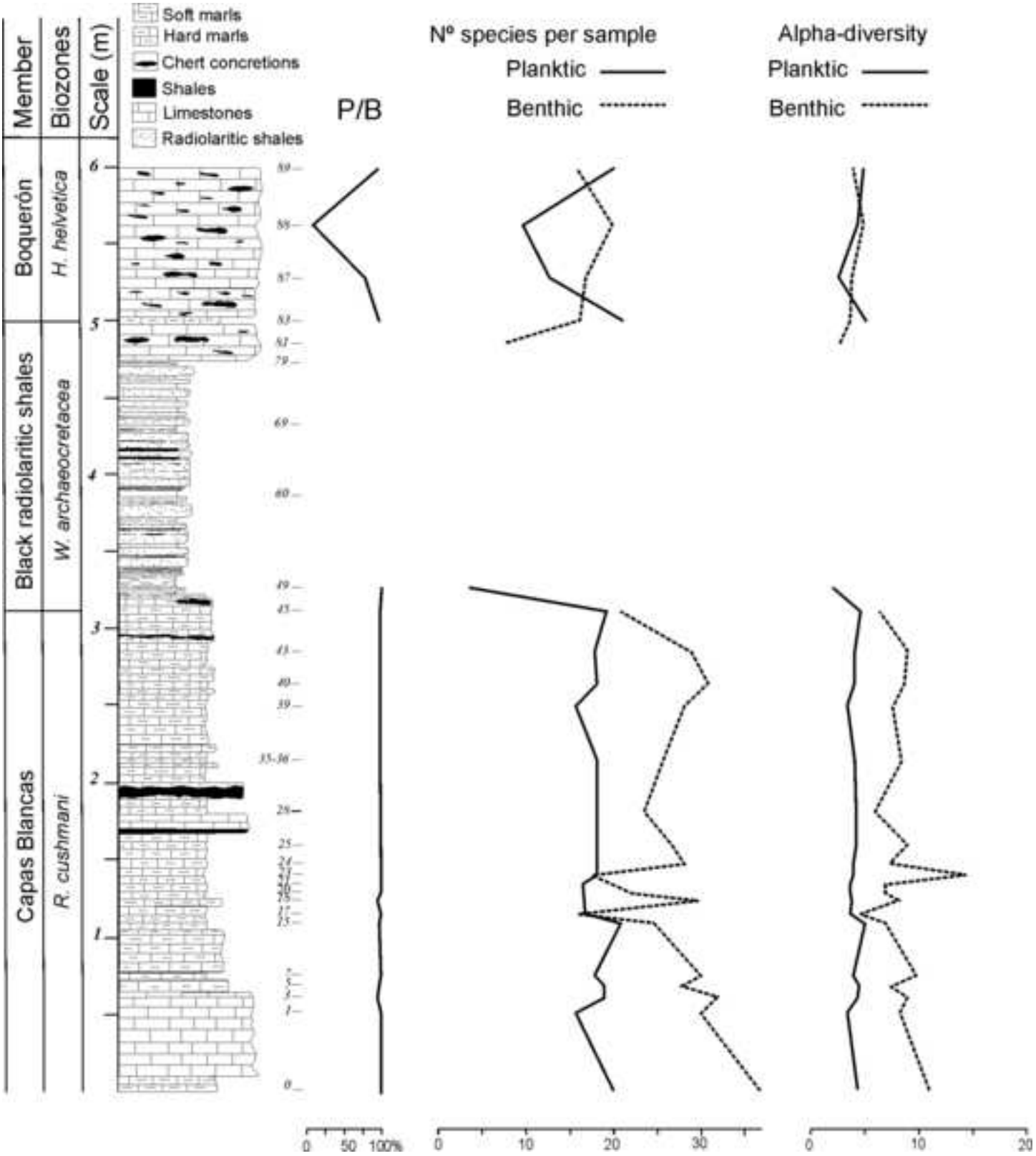

Figure 05
Click here to download high resolution image

Morphogroup	Genera	Habitat	Strategy	Requirements	
				Oxygenation	Trophic
Strongly keeled trochospiral	*Dicarinella* 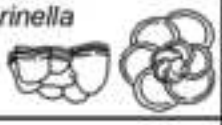	Intermediate-dweller	Intermediate	Oxygenated	Mesotrophic
	Parathalmanninella *Thalmanninella* 	Intermediate to deep-dweller	Specialist	Well-oxygenated	Oligotrophic
	Rotalipora 	Intermediate to deep-dweller	Specialist	Well-oxygenated	Oligotrophic
Weakly keeled trochospiral	*Helvetoglobotruncana* 	Intermediate to deep-dweller	Intermediate to specialist	Oxygenated to well-oxygenated	Oligotrophic to mesotrophic
	Praeglobotruncana *Marginotruncana* 	Intermediate-dweller	Intermediate	Oxygenated	Mesotrophic
Unkeeled trochospiral	*Hedbergella* 	Surface-dweller	Opportunist	Oxygenated to poorly-oxygenated	Eutrophic
	Shackoina 	Intermediate-dweller	Intermediate	Oxygenated to poorly-oxygenated	Mesotrophic to eutrophic
	Whiteinella 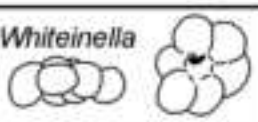	Surface-dweller	Opportunist	Oxygenated to poorly-oxygenated	Mesotrophic to eutrophic
Planispiral	*Globigerinelloides* 	Surface to intermediate-dweller	Opportunist to intermediate	Oxygenated to poorly-oxygenated	Mesotrophic to eutrophic
Biserial	*Heterohelix* *Globoheterohelix* 	Surface to intermediate-dweller	Opportunist	Oxygenated to poorly-oxygenated	Eutrophic
Triserial	*Guembelitria* 	Surface-dweller	Opportunist	Poorly-oxygenated	Eutrophic

Figure 06

Click here to download high resolution image

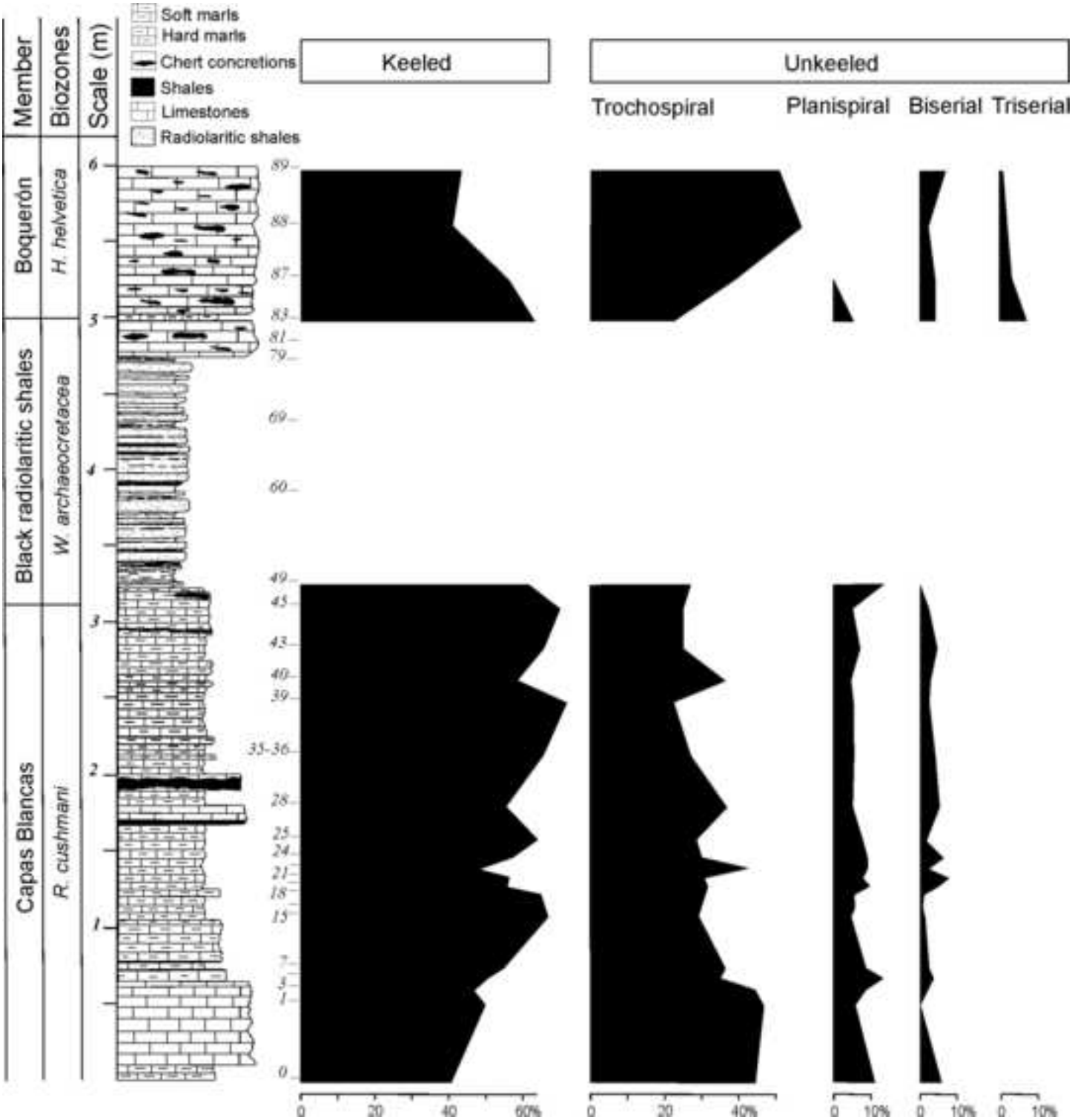

Figure 07a

Click here to download high resolution image

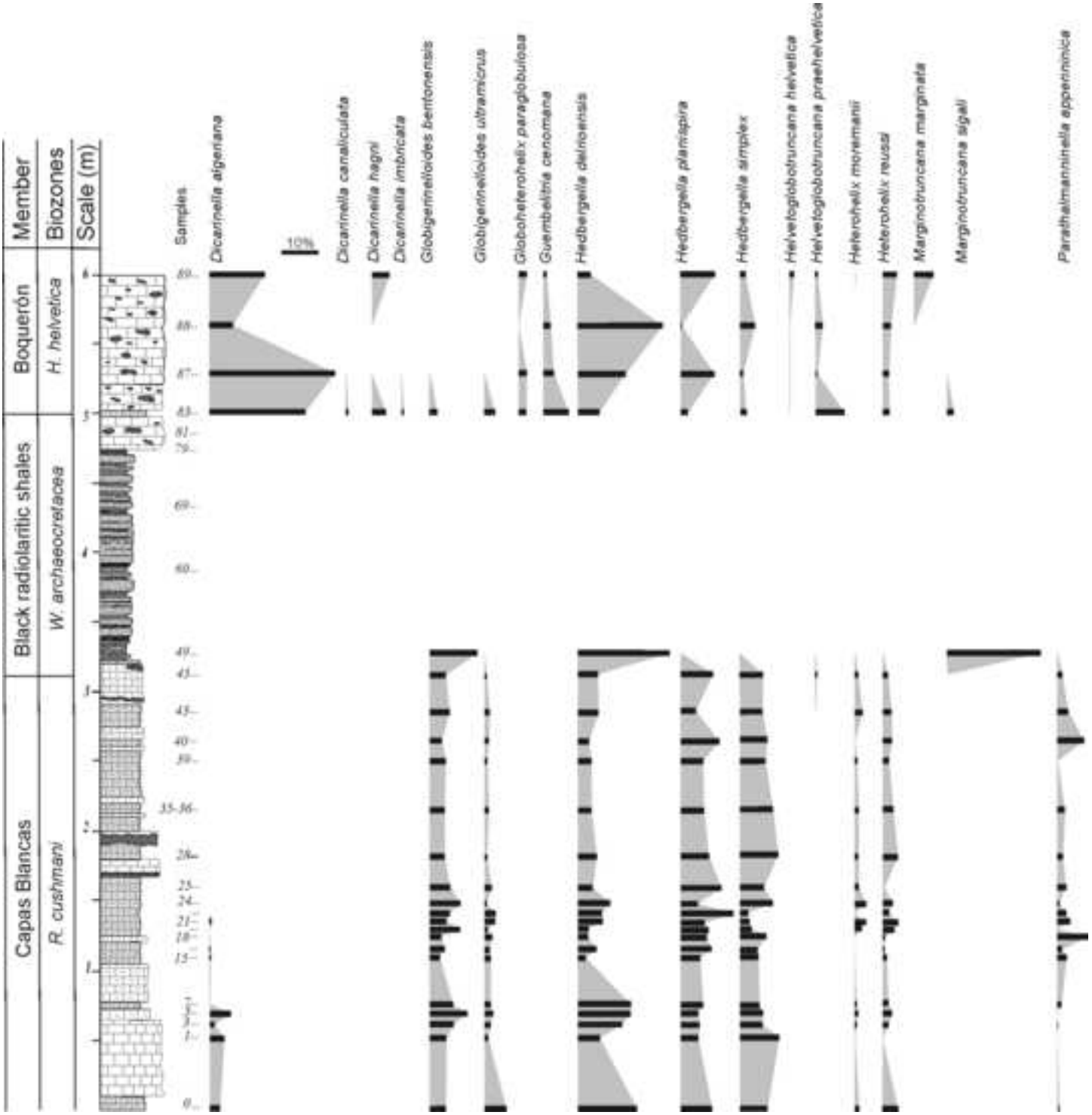

Figure 07b

Click here to download high resolution image

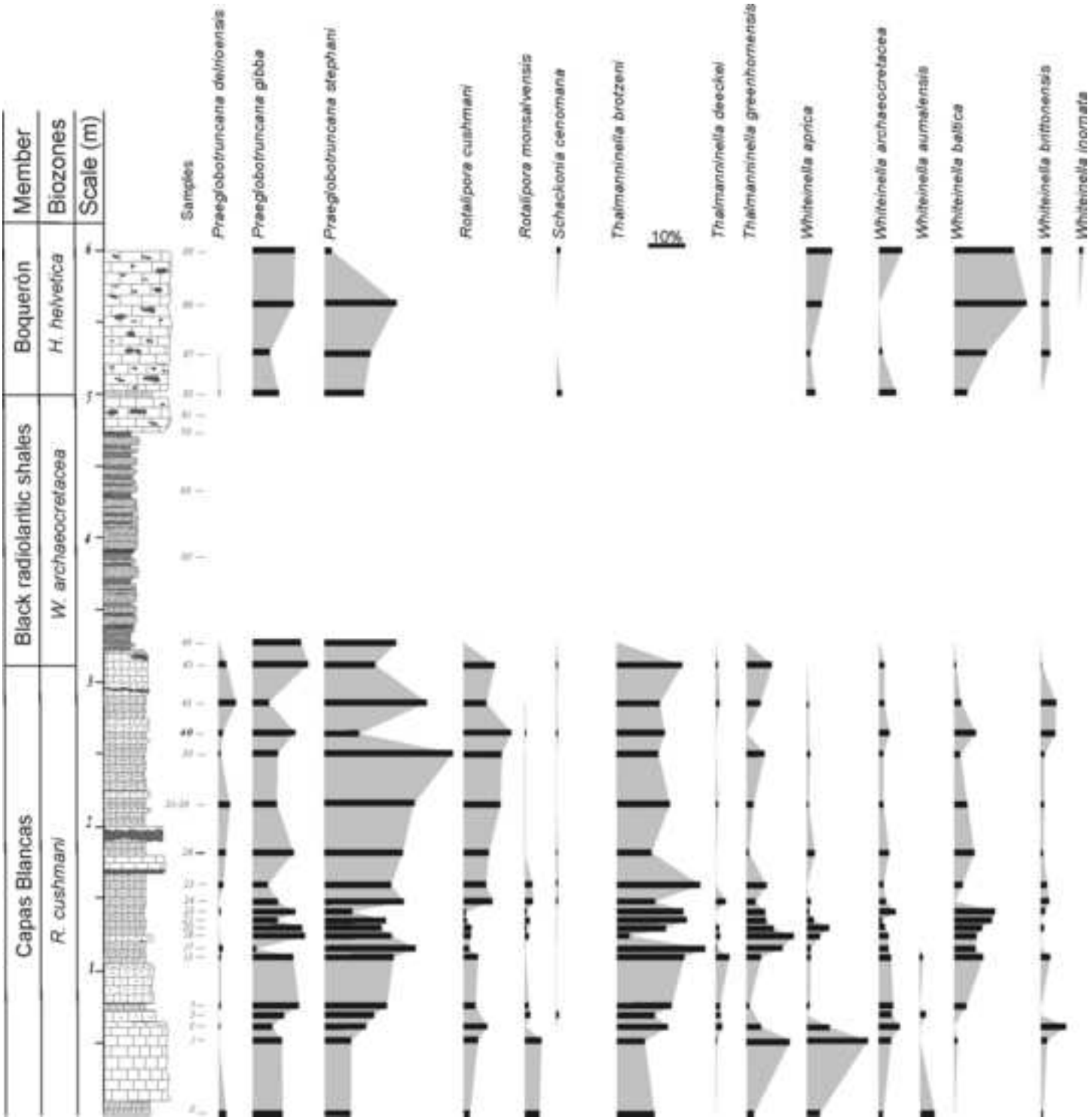

Figure 08
Click here to download high resolution image

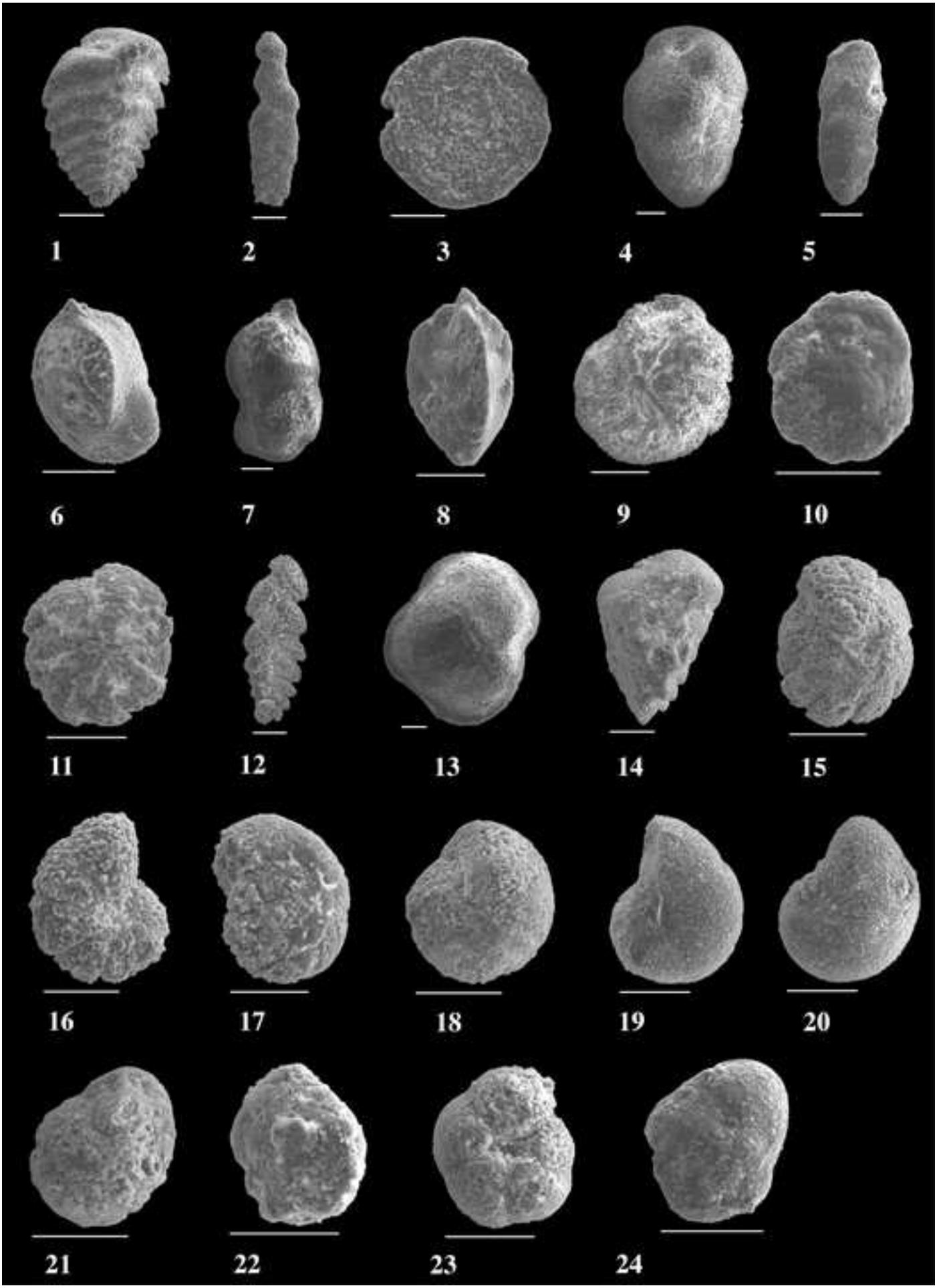

Figure 09a

Click here to download high resolution image

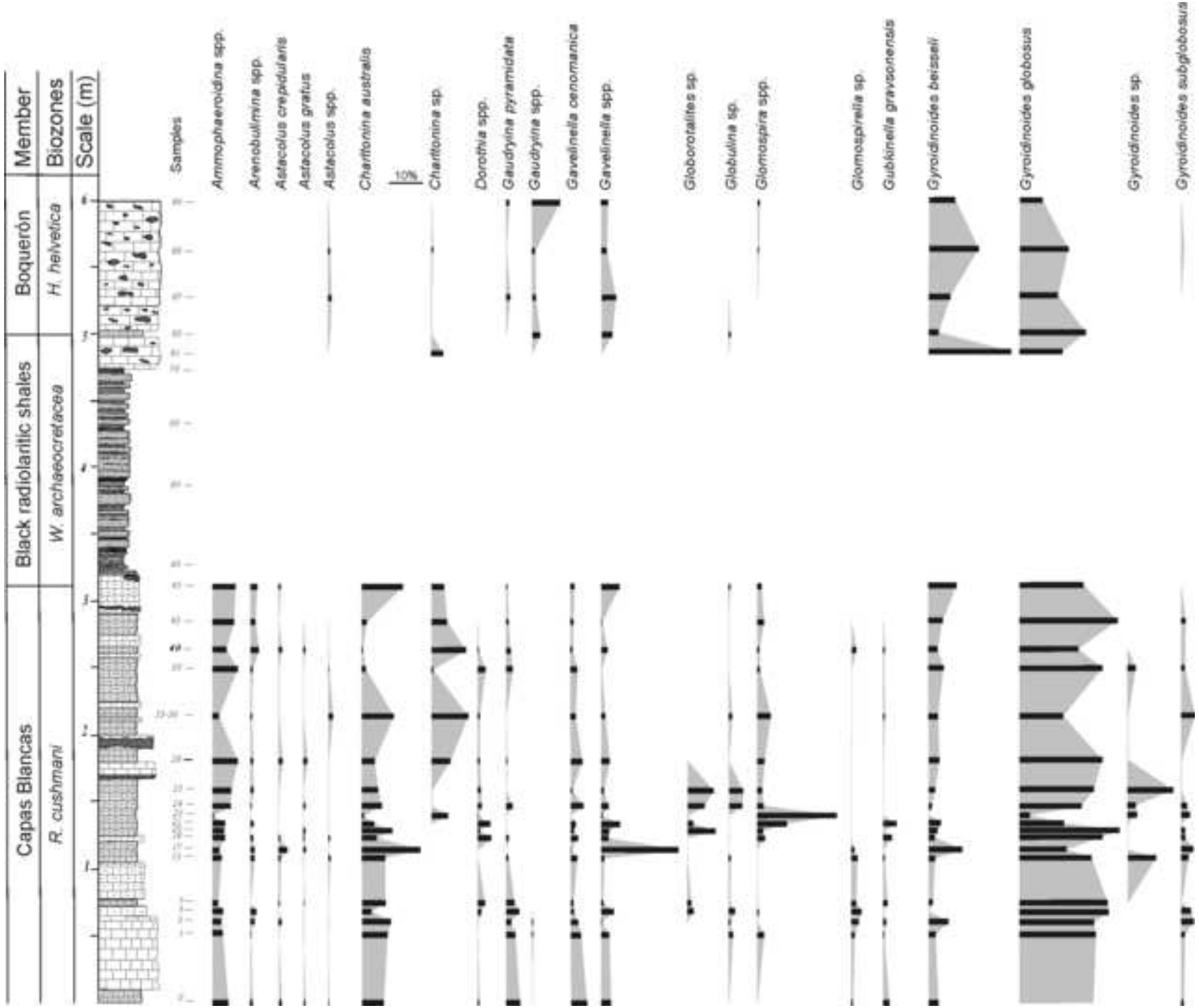

Figure 09b

Click here to download high resolution image

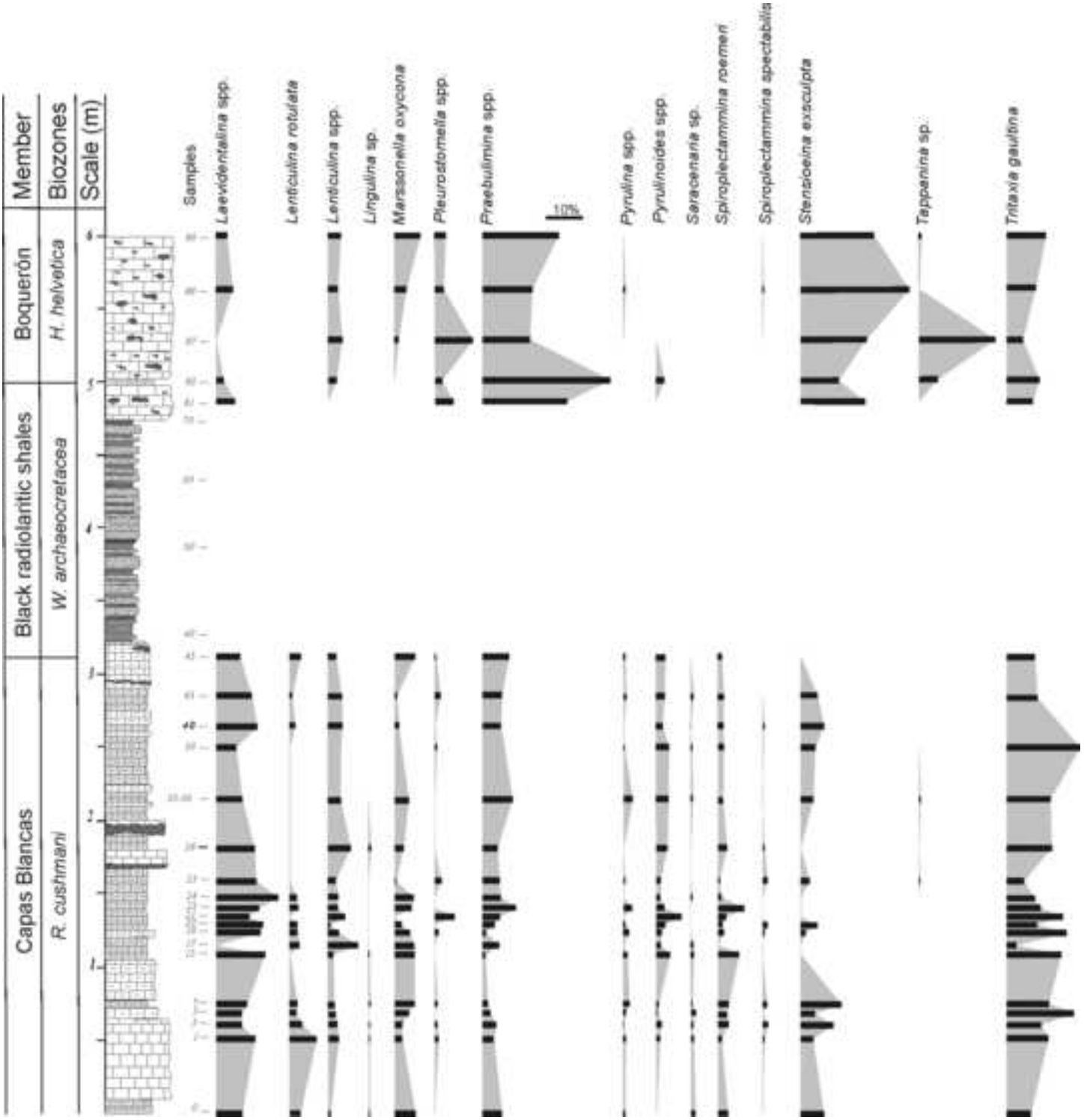

Figure 10

Click here to download high resolution image

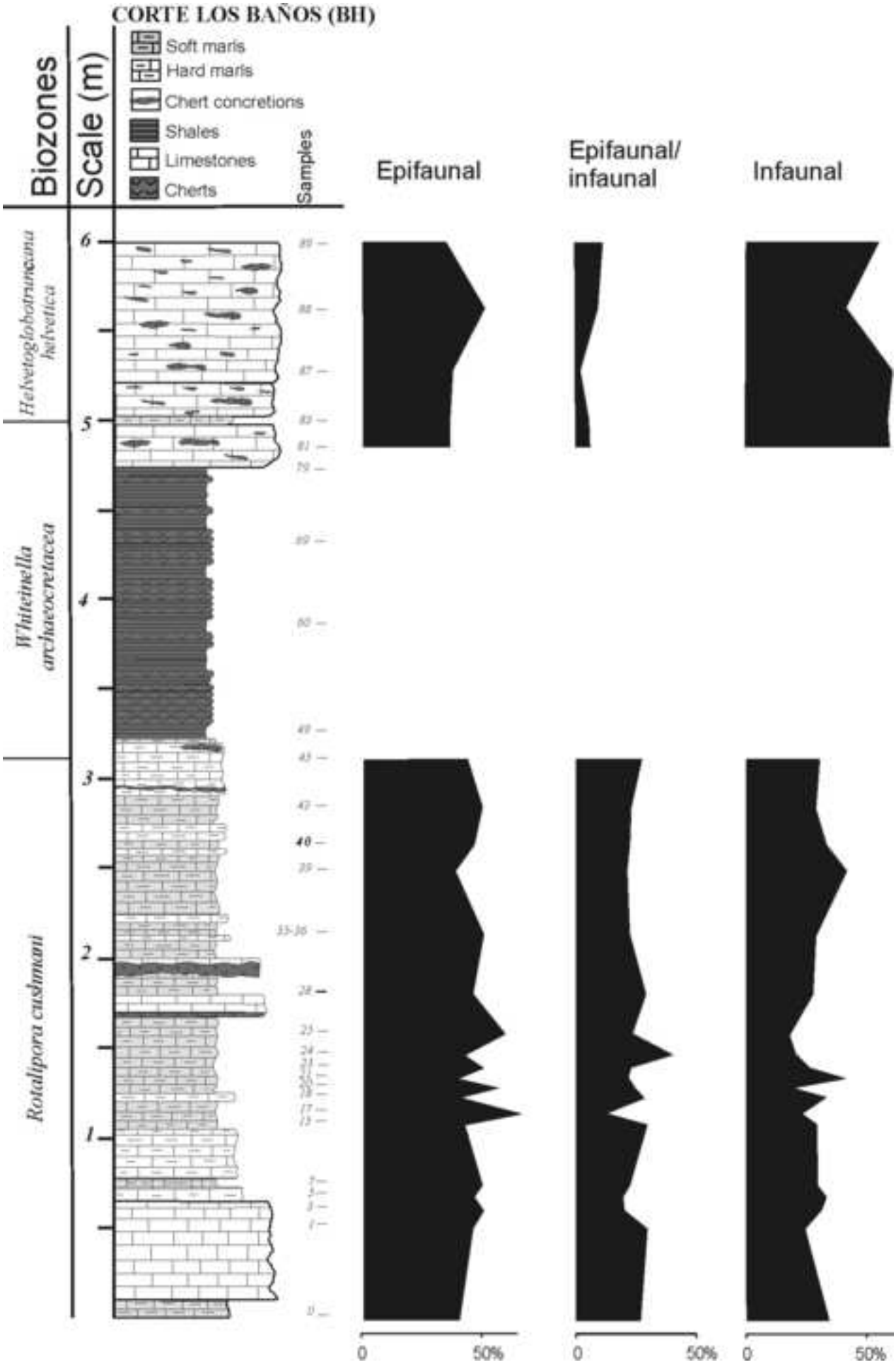

Figure 11

Click here to download high resolution image

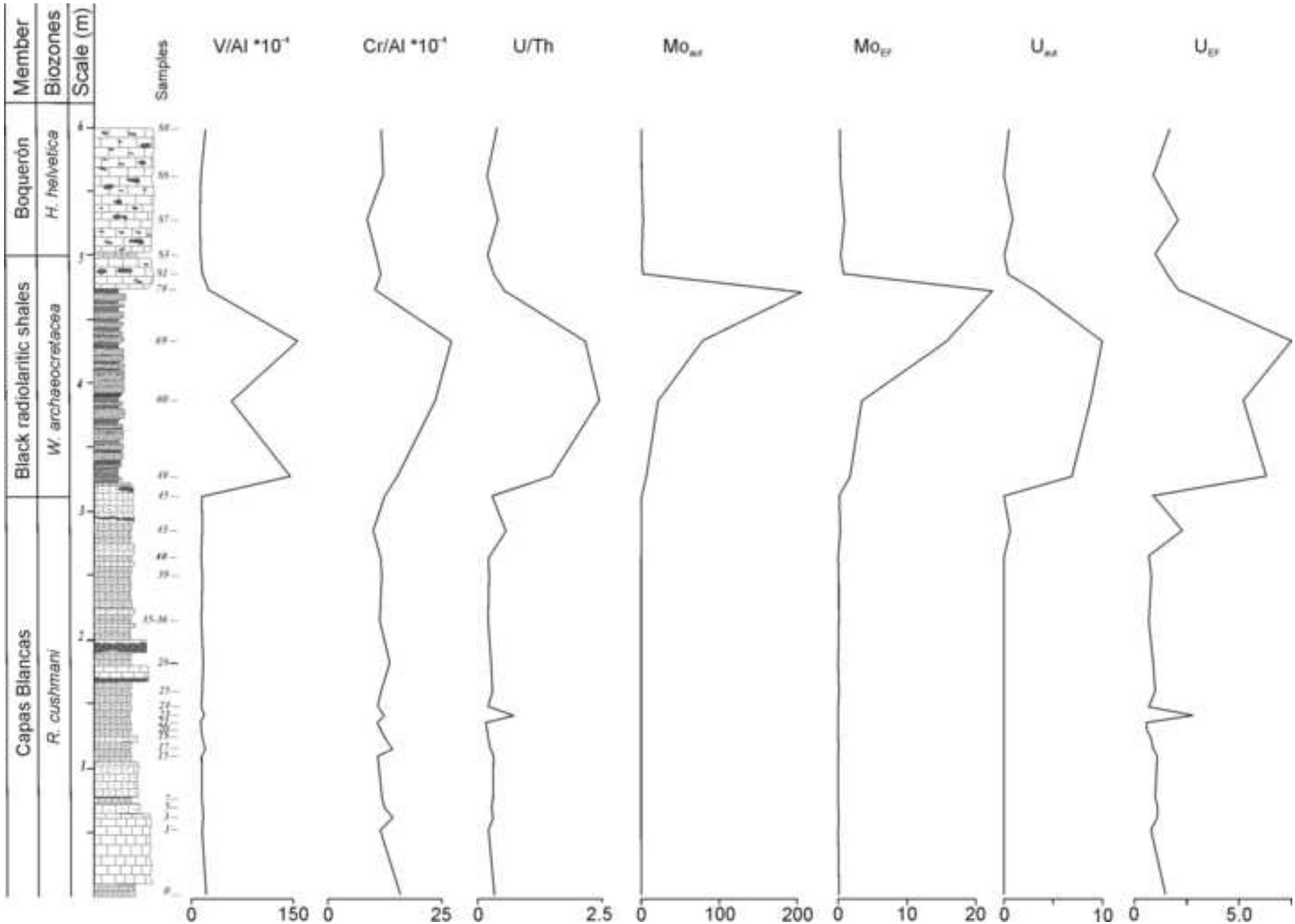

Figure 12

Click here to download high resolution image

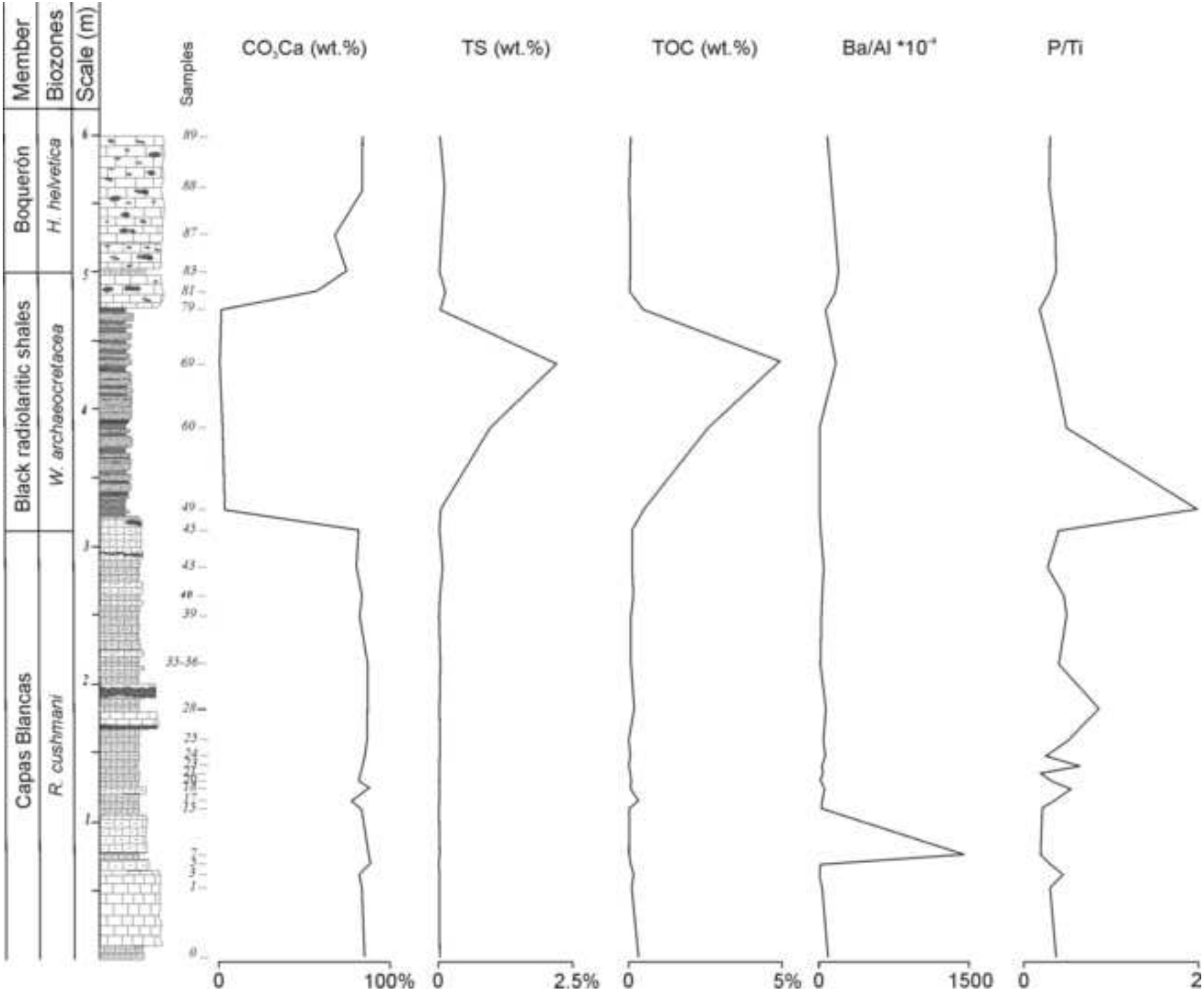

Figure 13

Click here to download high resolution image